Neuropharmacology 245 (2024) 109800

Contents lists available at ScienceDirect

Neuropharmacology

journal homepage: www.elsevier.com/locate/neuropharm

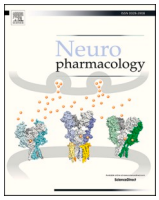

A paradigm for ethanol consumption in head-fixed mice during prefrontal cortical two-photon calcium imaging

Anagha Kalelkar [a,1], Grayson Sipe [b,1], Ana Raquel Castro E Costa [a], Ilka M. Lorenzo [a], My Nguyen [a], Ivan Linares-Garcia [a], Elena Vazey [c], Rafiq Huda [a,*]

[a] WM Keck Center for Collaborative Neuroscience, Department of Cell Biology and Neuroscience, Rutgers University – New Brunswick, 604 Allison Road, Piscataway, NJ, 08904, USA

[b] Department of Brain and Cognitive Science, Picower Institute for Learning and Memory, Massachusetts Institute of Technology, 43 Vassar Street, Cambridge, MA, 02139, USA

[c] Department of Biology, The University of Massachusetts Amherst, 611 North Pleasant Street, Amherst, MA, 01003, USA

ARTICLE INFO

Handling Editor: Bruno Frenguelli

Keywords:
Alcohol
Prefrontal cortex
Anterior cingulate cortex
Ethanol
Head-fixed
Binge drinking
Two-photon
Calcium imaging

ABSTRACT

The prefrontal cortex (PFC) is a hub for cognitive behaviors and is a key target for neuroadaptations in alcohol use disorders. Recent advances in genetically encoded sensors and functional microscopy allow multimodal *in vivo* PFC activity recordings at subcellular and cellular scales. While these methods could enable a deeper understanding of the relationship between alcohol and PFC function/dysfunction, they typically require animals to be head-fixed. Here, we present a method in mice for binge-like ethanol consumption during head-fixation. Male and female mice were first acclimated to ethanol by providing home cage access to 20% ethanol (v/v) for 4 or 8 days. After home cage drinking, mice consumed ethanol from a lick spout during head-fixation. We used two-photon calcium imaging during the head-fixed drinking paradigm to record from a large population of PFC neurons (>1000) to explore how acute ethanol affects their activity. Drinking exerted temporally heterogeneous effects on PFC activity at single neuron and population levels. Intoxication modulated the tonic activity of some neurons while others showed phasic responses around ethanol receipt. Population level activity did not show tonic or phasic modulation but tracked ethanol consumption over the minute-timescale. Network level interactions assessed through between-neuron pairwise correlations were largely resilient to intoxication at the population level while neurons with increased tonic activity showed higher synchrony by the end of the drinking period. By establishing a method for binge-like drinking in head-fixed mice, we lay the groundwork for leveraging advanced microscopy technologies to study alcohol-induced neuroadaptations in PFC and other brain circuits.

This article is part of the Special Issue on "PFC circuit function in psychiatric disease and relevant models".

1. Introduction

Binge drinking is defined by the National Institute on Alcohol Abuse and Alcoholism as a pattern of alcohol consumption leading to blood ethanol concentrations (BEC) of >80 mg/dL (Crabbe et al., 2011). Binge drinking poses significant health risks including severe potential acute effects such as bodily injury, automobile accidents, and death from overdose. Repeated episodes of binge drinking also lead to adverse consequences affecting the heart, liver, and other organ systems (Dawson et al., 2005). Moreover, binge drinking is a major risk factor for developing alcohol use disorder (AUD), a chronically relapsing condition characterized by compulsive alcohol seeking and consumption. Neural mechanisms that promote binge drinking and the neuroadaptations elicited by repeated alcohol intake remain incompletely understood but are important to resolve in order to identify novel therapeutic targets for curbing excessive drinking and the associated health burdens.

The prefrontal cortex (PFC) is an associative region of the brain with canonical roles in executive function and cognition, including decision making, attention, reward/punishment processing, social behavior, and

* Corresponding author.
E-mail address: rafiq.huda@rutgers.edu (R. Huda).
[1] Equal contribution.

https://doi.org/10.1016/j.neuropharm.2023.109800
Received 17 July 2023; Received in revised form 6 November 2023; Accepted 24 November 2023
Available online 4 December 2023

other functions (Alexander and Brown, 2011). Consistent with the association of AUD with dysfunction of these higher-order processes (Bechara et al., 2001; George and Koob, 2010; Ridderinkhof et al., 2002), the PFC is highly implicated in AUD in humans (Goldstein and Volkow, 2011; Wilcox et al., 2014) as well as in non-human primate (Jedema et al., 2011) and rodent models (Halladay et al., 2020; Pava and Woodward, 2014; Robinson et al., 2019; Salling et al., 2018). Significant evidence describes mechanistic changes in PFC structure and function following acute or chronic alcohol exposure (Cannady et al., 2021; Lu and Richardson, 2014), with changes typically assessed in separate cohorts of animals at various time points throughout the alcohol exposure paradigm. However, little is known about the effects of alcohol on the real time neurophysiology of individual neurons and neuronal networks in intact circuits of behaving animals voluntarily consuming alcohol. Moreover, understanding how neuronal processing in PFC networks on the sub-second time scale relates to voluntary drinking, and tracking this relationship across days and weeks of drinking, is crucial for identifying the key neuroadaptations underlying the development of AUD.

Research in preclinical animal models, wherein animals voluntarily consume ethanol to binge-like levels, has generated significant mechanistic information on the bidirectional relationship between neuronal activity and ethanol consumption (Holleran and Winder, 2017; Siciliano et al., 2015). Several paradigms have been used successfully for achieving binge-like BECs in animal models, including procedures for home cage drinking in mice (Crabbe et al., 2011; Rhodes et al., 2005). Though these settings represent more naturalistic contexts, they limit the technical approaches that can be used to measure and manipulate *in vivo* brain dynamics. By leveraging emerging tools for activity recordings and manipulations in freely behaving mice (for e.g., electrophysiology (Cannady et al., 2020; Linsenbardt and Lapish, 2015), fiber photometry (Gioia and Woodward, 2021; Liu et al., 2020) and chemogenetics (Dao et al., 2021; Giacometti et al., 2020; Rinker et al., 2017)), recent studies have identified how the molecular, cellular, and circuit properties of neurons and glia in defined brain circuits for reward, motivation, and stress both affect and are affected by binge-like consumption (Crabbe et al., 2011; Huynh et al., 2019; Rhodes et al., 2005; Simms et al., 2008; Sprow and Thiele, 2012; Thiele and Navarro, 2014). Parallel advances in high-density electrophysiological recordings (e.g., Neuropixels), multiphoton microscopy, and widefield calcium imaging now expand interrogation of brain function in awake, behaving animals across the spatial scale of information processing relevant for alcohol-related behaviors (Siciliano and Tye, 2019). These techniques allow functional activity and structural measurements of subcellular compartments (e.g., axons and dendrites), single cells (neuronal and non-neuronal glia cell bodies), and the network ensemble activity of hundreds to thousands of neurons simultaneously across multiple brain areas. Moreover, they open the possibility of longitudinally tracking the microscopic activity of single cells and macroscopic activity of individual brain areas across days to weeks of ethanol consumption, allowing for the systematic analysis of how neuronal activity changes with repeated ethanol intake. While these techniques are being explored in freely moving animals (Accanto et al., 2023; Juavinett et al., 2019), the most common experimental setups require head-fixation, and paradigms for voluntary drinking in head-fixed mice have not been characterized.

Here, we present a paradigm for voluntary, head-fixed ethanol drinking (HFD) as a modified extension of the well-studied "drinking-in-the-dark" (DID) paradigm (Rhodes et al., 2005; Thiele et al., 2014; Thiele and Navarro, 2014). Mice transfer binge-like drinking behavior from the classic DID paradigm in their home cages to head-fixation, thereby allowing alcohol studies with cutting-edge neuroscientific techniques that require head fixation (also see (Timme et al., 2024)). As an example application of this paradigm, we recorded PFC population activity with single-cell resolution using two-photon calcium imaging during head-fixed ethanol consumption. Drinking had heterogenous effects on single neuron activity at slow and fast time scales but did not significantly affect pairwise neuronal correlations. Together with traditional freely-moving paradigms, this new complementary approach will provide additional insights into the cellular- and circuit-specific mechanisms that contribute to the development and treatment of AUD.

2. Materials and methods

2.1. Animals

Behavioral experiments were performed on male and female C57/BL6J mice maintained on a reversed light/dark circadian cycle with *ad libitum* access to standard mouse chow and water. Mice of either sex were ~10 weeks at the start of behavioral experiments (mean 9.84, range 6–21 weeks). For two-photon calcium imaging experiments, animals expressed GCaMP6f under the CaMKII promoter and were generated by crossing the commercially available Camk2a-Cre (005359, Jackson) and Ai148D (030328, Jackson) mouse lines, both on a C57/Bl6 background. Imaging studies were done on ~ P60 male mice. Behavioral experiments were performed at Rutgers University and imaging experiments were done at MIT. All animal procedures were performed in strict accordance with protocols approved by the MIT Division of Comparative Medicine and Rutgers Comparative Medicine Resources and conformed to NIH standards.

2.2. Surgical procedures – headplate implant

Surgeries were performed under isoflurane anesthesia (4% induction, 1–3% maintenance). Body temperature was maintained at 37.5 °C via a heating pad integrated into the base of the stereotaxic frame and a temperature controller (53,800, Stoelting). Mice were given a subcutaneous injection of extended-release buprenorphine (3.25 mg/kg) before surgery to provide analgesia for up to 72 h post-surgery; meloxicam (10 mg/kg) was provided if additional analgesia was required during the recovery period. Anesthetized mice were head-fixed in a stereotaxic frame (51500D, Stoelting). Scalp hair was removed using a depilatory cream (Nair) and the scalp was disinfected using alternating scrubs with betadine and 70% ethanol solution. A portion of the scalp was removed and conjunctive tissues cleared after treatment with 3% hydrogen peroxide. The skull was abraded with a dental drill. A custom-designed headplate (eMachineShop) was placed over the skull and adhered in place using dental acrylic (Metabond, Parkell) mixed with black ink. Animals were then allowed to recover in their own cage with a warm water blanket and moistened food chow. Mice were singly housed for the remainder of the experiment and recovered from surgery for at least one week before beginning experiments.

2.3. Surgical procedures – chronic window implantation

The procedure for chronic window implantation was similar to headplate implantation as described in section 2.2, but a cranial window was implanted in addition to the headplate during the same surgery. Surgeries were performed under isoflurane anesthesia (3% induction, 1–3% maintenance) and body temperature was maintained at 37.5 °C using a temperature controller (ATC2000, World Precision Instruments). Animals were dosed with slow-release buprenorphine (0.1 mg/kg) prior to surgery, and meloxicam (1 mg/kg) every 24 h post-surgery for 72 h or until fully recovered. After exposing the scalp, a 3 mm diameter craniotomy was drilled centered over the left ACC/M2 region (from bregma, AP: 1.0 mm, ML: 1.0 mm). A chronic cranial window, consisting of a 5 mm diameter coverslip glued to two 3 mm coverslips (Warner Instruments) with optical UV-cured adhesive (61, Norland) was then implanted. The window was carefully lowered with the 5 mm coverslip on top and firmly held in the craniotomy using the stereotax arm and adhered to the skull using dental acrylic mixed with black ink (Metabond, Parkell). Once the dental acrylic had cured around the cranial window, the headplate was implanted using dental acrylic as described in 2.2. 3 mice in the 1-cycle paradigm received intracranial injection of

an AAV virus expressing CaMKII-ChR2 in the ACC and were implanted with a bilateral optic fiber cannula above the injection. Data is presented from sessions before any optogenetic manipulations.

2.4. Drinking in the dark (DID) paradigm

Following recovery from surgery, mice were acclimated to ethanol consumption using the drinking in the dark (DID) paradigm. Mice for behavioral experiments were given 1 or 2 cycles of DID. For each DID cycle, mice had access to ethanol for 2 h on days 1–3 and for 4 h on day 4; no ethanol was available on days 5–7. Mice were weighed daily, and their water bottles were replaced with 10 mL drinking bottles fitted with a sipper tube (Amuza) containing 20% ethanol (v/v) diluted in the mouse drinking water 3 h into their dark phase (ZT15). Tubes were weighed before being placed in each cage. A control cage without any mice was also fitted with an ethanol drinking bottle with a sipper tube to account for evaporation. Mice were then left alone for the duration of the DID period to consume the ethanol solution. Afterwards, ethanol drinking bottles were removed, weighed, and regular drinking water bottles returned. The amount of ethanol consumed was calculated by subtracting the final weight from the initial weight of each tube to get a session difference. The control tube difference was then subtracted from each mouse tube difference, and then consumption computed as ethanol consumed (g) per weight of the animal (kg). Mice for two-photon imaging experiments were similarly acclimated to ethanol consumption except they performed DID for 13 consecutive days with ethanol access for 3 h on each day.

2.5. Head-fixed drinking paradigm

The rig for head-fixed drinking (HFD) experiments was custom designed using parts from Thorlabs. After DID exposure, mice for behavioral experiments were habituated to head-fixation in 30-min sessions over 2 days. For the two-photon imaging experiments, mice were habituated to head-fixation during the last 5 days of DID drinking. Animals were head-fixed on an elevated platform with a lickspout delivering 20% ethanol (v/v) in mouse drinking water positioned within easy access for licking. The lickspout was made from a brass tube (3.97 mm diameter, 8128, K&S Precision Metals) for two-photon experiments or a blunt 13-gauge needle (McMaster-Carr) for behavioral experiments. For lick detection, the brass tube was wrapped with conductive wire and connected to a capacitive sensor (P1374, Adafruit) integrated to a breadboard. Alternatively, the 13-gauge needle was connected via a wire to a transistor-based electronic circuit for lick detection (Huda et al., 2020; Slotnick, 2009). In either case, contact of tongue to the spout generated a voltage signal that was fed to an Arduino board (Uno Rev3, A000066, Arduino) as an analog input and recorded via custom MATLAB scripts. Ethanol delivery was initiated by custom MATLAB scripts that sent a digital signal via the Arduino to toggle a transistor on the breadboard (IRF520PBF, Digi-Key) and open a 12 V solenoid (VAC-100 PSIG, Parker or 161K011, NResearch).

Ethanol solution was maintained in a graduated syringe and gravity fed into the solenoid to deliver a small drop with each trigger (~8 μL for two-photon experiments; ~5 μL for behavioral experiments). Ethanol delivery was calibrated by opening the delivery solenoid for a set duration over multiple deliveries (for e.g., 40ms x 10 deliveries) and then recording the dispensed total volume using the graduated syringe. We used 10+ deliveries to account for decreased accuracy in measuring small volumes. After measuring multiple durations (for e.g., 10 deliveries at 40, 60, 80, 100, and 120ms) and recording the dispensed total volumes, a line was fit to the sampling points and saved as a calibrated look-up function. To deliver 5 μL in each drop, we found the solenoid time on the look-up function that corresponds to this volume. Calibration look-up functions were generated daily before experiments. Following each session, total ethanol delivered was compared between the graduated syringe and the calculated trigger volume to ensure accurate quantification of total ethanol delivered (for detailed example circuit diagram, see Fig. 1). In a subset of experiments, we placed a weigh boat underneath the spout to catch and weigh any spilled liquid (2-cycle paradigm). For these experiments, consumption values were adjusted for the spilled liquid.

Each HFD session consisted of a 10-min baseline pre-drinking period followed by 20-min of ethanol drinking, which was arbitrarily split into early and late drinking blocks for data acquisition and analysis, and consisted of the first and second 10-min of ethanol drinking, respectively. We head-fixed the animal and situated the spout in front of the mouth at the start of the session. The spout was aligned so it did not touch the animal, but a protrusion of the tongue would be registered as a lick. Spout placement was inspected visually from multiple angles and via an infrared camera. Mice were free to lick the spout during the pre-drinking block, but licking did not deliver any liquid. Following the pre-drinking block, animals underwent two subsequent 10-min drinking blocks in which licking the spout could deliver a drop of ethanol. We used a random interval schedule with a pseudorandom delay between drop deliveries (exponential distribution with a 10s mean and cut-offs at 5s and 20s). If the animal licked at least once since the prior delivery (or the beginning of the session for the first delivery), a drop of ethanol solution was dispensed. Otherwise, the delay was increased by 1s until a lick was made. Hence, the animal had to continually lick to trigger ethanol delivery. This design promoted licking of the spout in order to obtain more ethanol, thereby limiting unconsumed ethanol delivery. Moreover, the self-paced design allowed us to assess the animal's level of engagement with ethanol by quantifying the number of drops that were triggered. An infrared camera and infrared illumination source were used to record pupil responses during the paradigm; these data are not included in this study and may be reported elsewhere.

2.6. Measurement of blood ethanol concentration

Blood ethanol concentration (BEC) for behavioral experiments was quantified with an Analox AM1 Analyzer using plasma separated from tail bloods. Mice were given additional HFD sessions at the end of the experiment for collecting tail bloods. For two-photon imaging experiments, BEC was quantified using a previously described assay (Prencipe et al., 1987). Immediately after the last drinking session, animals were rapidly anesthetized by isoflurane, decapitated, and whole trunk blood collected in tubes lined with EDTA (BD Microtainer, 365,974, Becton, Dickinson and Company) and placed on ice. Whole blood was then centrifuged at 3000×*g* for 10 min at 4 °C. Separated plasma was then aliquoted and immediately stored at −80 °C for further analysis. Quantification of BEC was performed using a colorimetric assay as previously described. Ethanol standards and plasma samples were diluted in sample reagent (all reagents obtained from Millipore Sigma): 100 mM KH_2PO_4 (P3786), 100 mM K_2HPO_4 (P3786), 0.7 mM 4-aminoantropyrine (A4382), 1.7 mM chromotropic acid (27,150), 50 mg/L EDTA (E4884), and 50 mL/L Triton X100 (X100). Working reagent was created by mixing alcohol oxidase from *Pichia* (5kU/L, A2404) and horseradish peroxidase (3kU/L, 77,332) with sample reagent and mixed with samples on a 96-well plate. Following 30 min of incubation at room temperature, the samples and standards were read on a standard plate reader (iMark, Bio-Rad Laboratories) at 595 nm. Samples and standards were run 6x in parallel and BEC calculated according to the standard curve.

2.7. Two-photon calcium imaging

GCaMP6f fluorescence from neuronal somas was imaged through a 16x/0.8 NA objective (Nikon) using resonance-galvo scanning with a Prairie Ultima IV two-photon microscopy system. Image frames were 480 × 240 pixel resolution acquired at 64 Hz with 4-frame averages resulting in an effective frame rate of 16 Hz. Excitation light at 900 nm was provided by a tunable Ti:Sapphire laser (Mai-Tai eHP, Spectra-

Physics) with ~10–20 mW of power at sample. Emitted light was filtered using a dichroic mirror and collected with GaAsP photomultiplier tubes (Hamamatsu). Layer 2/3 GCaMP6f-expressing neurons were imaged with 1.5x optical zoom, 120–200 μm below the brain surface. Neuronal activity in the anterior cingulate cortex (ACC) was collected at the following coordinates: ~0.5 mm AP, ~0.5 mm ML.

2.8. GCaMP6f fluorescence signal processing

We used the software Suite2P (Pachitariu et al., 2017) for semi-automatic detection of neuronal somas from calcium imaging movies. Movies from the three imaging blocks were concatenated together and the non-rigid translation function in Suite2P was used to correct for x-y translations that may have occurred between blocks. Suite2P detects neuronal regions of interest (ROI) by clustering neighboring pixels with similar fluorescence time courses. Moreover, it provides for each detected neuron a neuropil mask which surrounds the detected ROI and excludes other detected neuronal ROIs. The automatically detected ROIs were manually curated using the GUI such that ROIs without clear structural evidence for neuronal somas were rejected and neurons missed by the algorithm were added manually.

To minimize the contribution of the neuropil signal to the somatic signal, corrected neuronal fluorescence at each time point t was estimated as $F_t = F\_soma_t - (0.3 \times F\_neuropil_t)$ (Chen et al., 2013). The DFF ($\Delta F/F$) for each neuron was calculated as $\Delta F/F(t) = F(t) - F_0)/F_0$, where F_0 represents the mode of the distribution of fluorescence values (estimated using the MATLAB function 'ksdensity'). The resulting DFF trace was z-scored. We identified individual calcium events as transient increases in the z-scored DFF signal. Using the 'findpeaks' function in MATLAB, we detected events with minimum peak prominence of 2.5 z-scored DFF and minimum width of 3 imaging frames (~200ms) at half-height of the event peak. All analyses either used the z-scored DFF or detected calcium event frequency and amplitude.

2.9. Analysis of change in neuronal activity with ethanol consumption

To determine how drinking affects ACC activity relative to before drinking, in later imaging sessions we introduced a 10 min pre-drinking imaging block in which animals were allowed to lick the spout but no ethanol was delivered (note that the pre-drinking block was included for all behavioral experiments). We analyzed data from drinking sessions with imaging during both pre-drinking and drinking blocks. We had 13 such sessions from 4 male mice, which were included in the analysis of pre-drinking activity. 2 sessions had poor quality imaging data in the late drinking block and hence were excluded from the analysis.

We tested how ethanol consumption affects neuronal activity over the slow time scale of minutes across the entire imaging session. While one strategy is to compare inter-event intervals between pre-drinking and drinking blocks, we reasoned that the sparse cortical activity observed in individual blocks would be a limiting factor and produce false negatives. Hence, we used a shuffle test. This test circularly shifted traces of detected calcium events in time by a random amount in intervals of 30s, thus maintaining the local temporal structure of activity while randomizing the time at which it occurred. We reiterated this process 1000 times for each neuron. On every iteration, we computed the difference in event frequency between pre-drinking and 1) the first drinking block; and 2) the second drinking block. This allowed us to generate null distributions for the difference in event frequency expected by chance given the overall activity level of the neuron. The two-tailed p-value for each drinking block was computed as the proportion of activity changes in the null distribution that were as or more extreme than the experimentally observed change on either side of the distribution. Neurons with $p < 0.05$ for either drinking block were considered significant and classified as tonic increased or tonic decreased neurons.

We also tested how individual ACC neurons were modulated on a faster time scale. We aligned neuronal activity to the time of first lick after ethanol delivery and compared responses before and after delivery using a two-tailed Wilcoxon signed-rank test to identify phasic increase and decrease neurons. Neurons with $p < 0.05$ were considered significant. Activity was shuffled by randomly permuting the timing of detected calcium events in trial-aligned data.

For some analyses, we computed the mean session activity of simultaneously recorded neurons in 2-min bins during the 20-min drinking period (all neurons or subgroups of neurons). Activity shuffling was performed by randomly permuting mean session activity across time bins.

2.10. Pairwise neuronal correlation analysis

We assessed the effect of ethanol consumption on Pearson correlations between the z-scored DFF traces for all unique pairs of neurons in each recording session. In some analyses, we computed pairwise correlations between unique pairs of neurons with significant activity modulation during the drinking period. To control for the influence of ethanol deliveries/consumption, we also computed pairwise correlations after excluding neuronal activity 10s following ethanol deliveries. Correlations were computed using the last 5 min of the pre and late drinking blocks.

3. Results

3.1. A paradigm for ethanol consumption in head-fixed mice

We first acclimated mice to ethanol consumption (20% v/v in standard drinking water) in their home cages using the 'drinking in the dark' (DID) paradigm which promotes binge-like levels of ethanol consumption. Each cycle (week) of DID consisted of ethanol access for 2 h on days 1–3 followed by 4-h access on day 4 (Fig. 1A and B). After completion of DID drinking, mice were habituated to head-fixation for 2–3 days. We tested two experimental designs for assessing head-fixed drinking, with one group receiving 1 cycle of DID and the other group receiving 2 cycles of DID (Fig. 1A). For both groups, DID was followed by head-fixed drinking (HFD). This allowed us to assess how home cage drinking history affects head-fixed drinking. Moreover, in a subset of mice we assessed head-fixed consumption of 3% sucrose to compare drinking patterns with ethanol.

We custom designed software and hardware to assess ethanol consumption behavior in head-fixed mice. Liquid delivery was controlled via a solenoid valve, which was calibrated daily to deliver ~5 μL drops via a lick spout (Fig. 1C). The software controlled liquid delivery such that drops were dispensed with a pseudorandom delay between 5 and 20s with a mean delay of 10s (Fig. 1D). The system monitored the licking behavior in real-time to deliver drops only if the animal licked at least once since the previously delivered drop. Liquid delivery was delayed by 1s until the animal made at least one lick (Fig. 1D). This design minimized delivery of unconsumed drops of ethanol and allowed mice to self-pace their consumption.

Mice were head-fixed for 30 min on each day of HFD sessions. We positioned the spout in close proximity to the mouth to facilitate licking and consumption. The first 10 min constituted the pre-drinking block during which no ethanol was delivered (Fig. 1B). We included this block for future experiments to allow quantification of neuronal activity and/or physiological parameters in the absence of ethanol. Mice could consume ethanol during the subsequent 20-min arbitrarily split into 1st and 2nd 10-min blocks. We designed our HFD paradigm such that ethanol delivery is contingent on licking and consumption. Rarely, we observed spilled liquid from the spout. We investigated this issue in the 2-cycle cohort by weighing spillage of unconsumed liquid from the spout. The average spillage was minimal; we observed spillage in 3 sessions across 55 sessions from 15 mice. We quantified blood ethanol concentration (BEC) from tail blood collected from a subset of mice after completion of HFD sessions. There was a linear relationship between

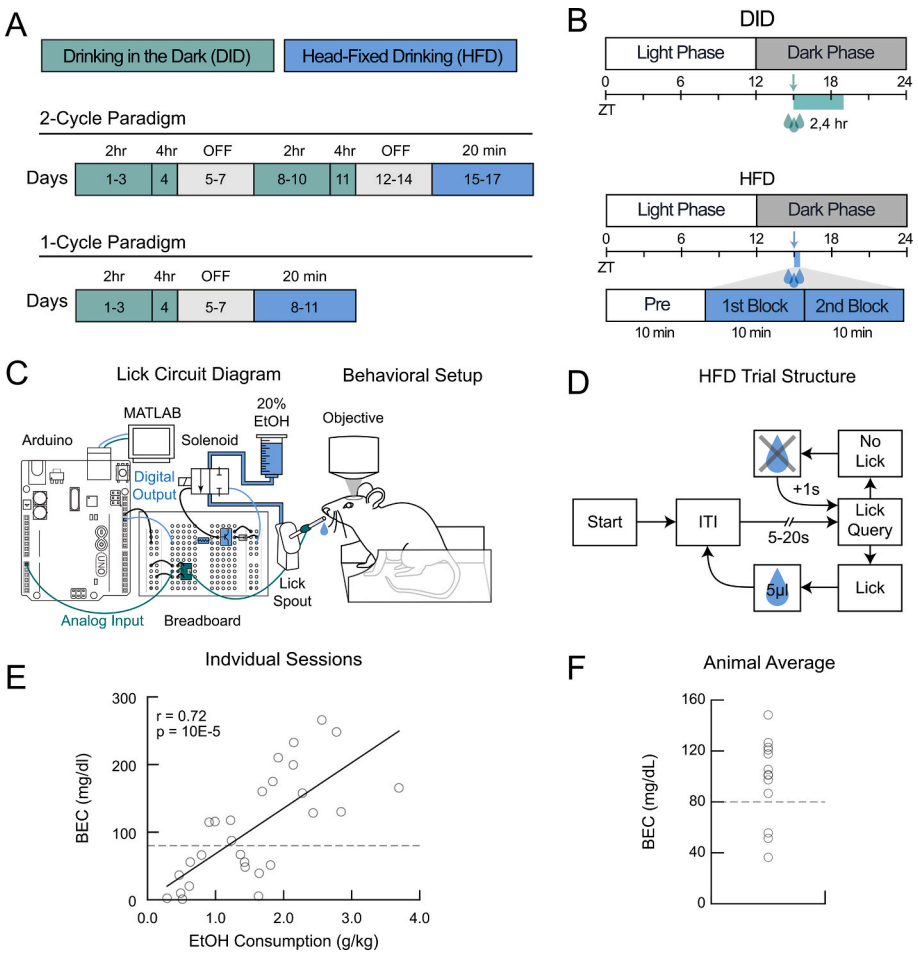

Fig. 1. Paradigm for head-fixed ethanol consumption. (A) Mice first were acclimated to ethanol consumption using either 1 or 2 cycles of the 'drinking in the dark' (DID) paradigm with access to alcohol for 2 or 4 h before undergoing head-fixed drinking (HFD) with access to alcohol for 20 min. **(B)** Mice started home cage drinking 3 h into the dark phase of their circadian cycle. Head-fixed drinking started at the same time and consisted of three 10-min blocks. A pre-drinking baseline block was followed by early and late drinking blocks. **(C)** Custom electronic circuit used for liquid delivery and lick detection during head-fixed drinking on a custom behavioral setup. **(D)** Trial structure for head-fixed drinking paradigm. **(E)** Relationship between head-fixed ethanol consumption and blood ethanol concentration quantified from plasma isolated from tail blood (2–4 sessions from each of 7 male and 6 female mice). **(F)** Session-averaged blood ethanol concentration for 13 mice.

consumption on single HFD sessions and BEC (Fig. 1E). Session-averaged consumption for individual mice showed pharmacologically relevant BEC levels for most mice (Fig. 1F). Hence, head-fixed mice consume ethanol to binge-like levels.

3.2. Comparison of home cage and head-fixed ethanol consumption

Overall, mice in both the 2-cycle and 1-cycle cohorts consumed more ethanol during the 4-hr DID session compared to HFD (Fig. 2A–D). However, normalizing total consumption by duration of the session showed the opposite pattern, with a substantially higher drinking rate during HFD than during DID (Fig. 2E, G). Hence, mice consume more ethanol per unit of time during HFD. Previous work shows sex differences in DID home cage ethanol consumption, with female C57/BL6J mice consuming more ethanol than males (Radke et al., 2021). We found a similar sex difference in head-fixed drinking, with females drinking more than males in both cohorts (Fig. 2F, H). Comparing sex-specific consumption in the two HFD paradigms using a two-way ANOVA showed a significant main effect of sex ($F(1,26) = 16.84$, $P = 4 \times 10^{-4}$) but not for type of paradigm ($F(1,26) = 2.43$, $P = 0.13$). There was no interaction between sex and HFD paradigm ($F(1,26) = 0.23$, $P = 0.64$). Hence, mice consumed similar amounts of ethanol during HFD regardless of 1 or 2 weeks of DID ethanol exposure.

We observed substantial across-animal and across-session consumption variability during HFD (Supp. Fig. 1A). We compared variability during DID and HFD consumption to test if head-fixation uniquely contributes to consumption variability. Variability was calculated as the coefficient of variation using consumption values on 3 days of DID (2-hr sessions) and first 3 days of HFD. For both cohorts, the variability across mice was similar for average ethanol consumption during DID and HFD (Fig. 2I, K). Moreover, the mean across-session variability was also similar between DID and HFD (Fig. 2J, L). Therefore, consumption variability in the head-fixed paradigm likely represents biological variability in ethanol consumption behavior.

The addition of quinine to ethanol is often used to assess aversion-resistant drinking as a preclinical model of compulsive-like ethanol intake (Radke et al., 2021). We examined aversion-related modulation of head-fixed drinking in the 1-cycle group by adulterating the ethanol solution with increasing concentrations of quinine over 4 days after standard HFD (0.25 – 1 mM in 0.25 mM increments; Supp. Fig. 1B). As expected, there was a significant decrease in HFD ethanol consumption with quinine adulteration (Supp. Fig. 1C). These results suggest that the HFD paradigm is suitable for studying neural correlates of aversion-resistant drinking (also see Timme et al., 2024).

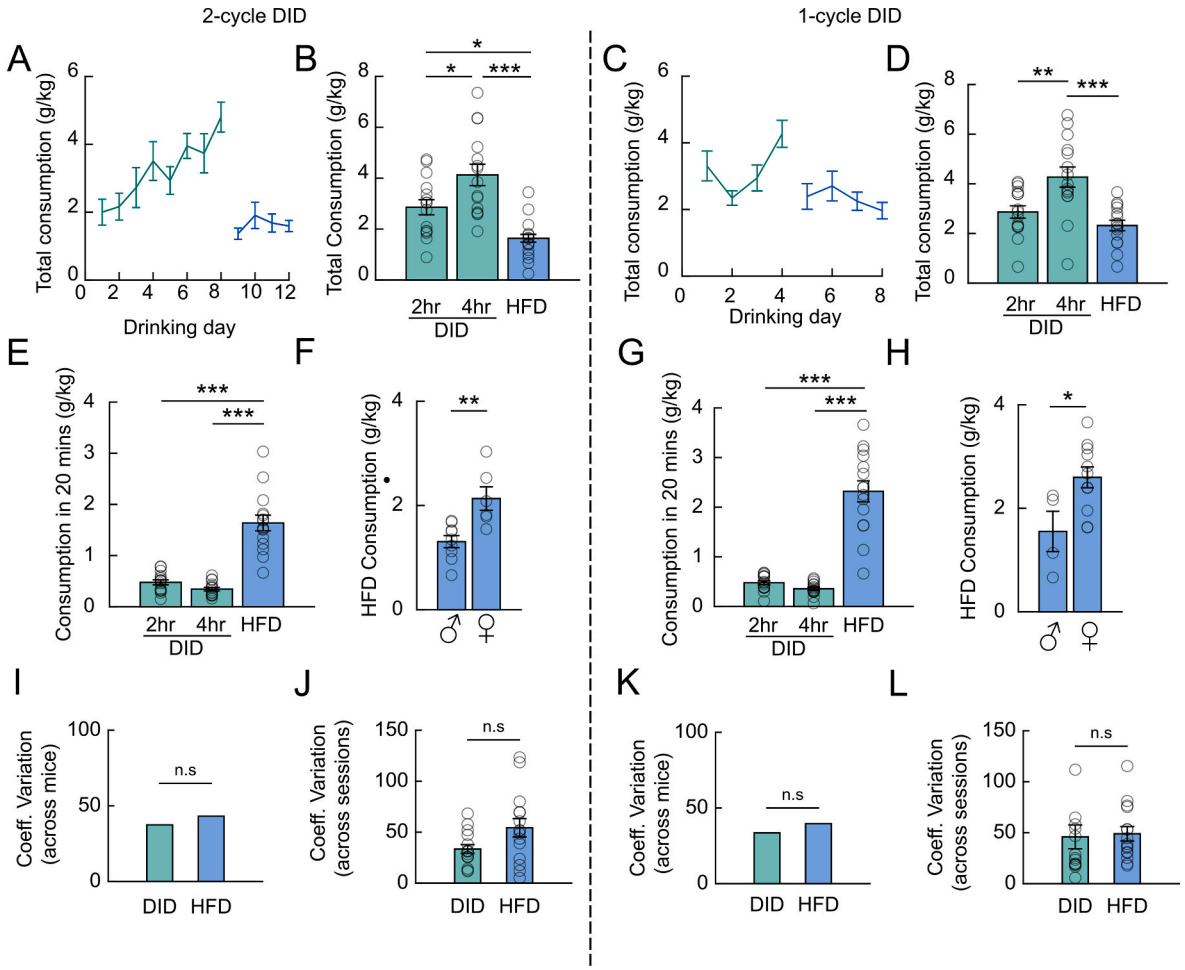

Fig. 2. Comparison of home cage and head-fixed ethanol consumption. (A) Total ethanol consumption (g/kg) during home cage (green) and head-fixed (blue) drinking for mice in the 2-cycle paradigm. **(B)** Mean total consumption during 2-hr DID, 4-hr DID and 20 min of HFD (n = 15 mice; one-way ANOVA main effect of paradigm type, $F(2,42) = 16.15$, $P = 6.0e^{-6}$; Tukey HSD multiple comparisons, 2hr vs. 4hr: P = 0.016, 95% C.I. = [-2.33, −0.20]; 2hr vs. HFD: P = 0.021, 95% C.I. = [0.16, 2.29]; 4hr vs. HFD: $P = 3e^{-06}$, 95% C.I. = [1.43, 3.55]. **(C)** Mean ethanol consumption during the 1-cycle paradigm. **(D)** Comparison of total consumption during 2-hr DID, 4-hr DID, and HFD drinking for 1-cycle paradigm (n = 15 mice; one-way ANOVA main effect of paradigm type, $F(2,42) = 11.22$, P = 0.0001; Tukey HSD multiple comparisons, 2hr vs. 4hr: P = 0.0053, 95% C.I. = [-2.44, −0.37]; 2hr vs. HFD: P = 0.41, 95% C.I. = [-0.49, 1.58]; 4hr vs. HFD: P = 0.0001, 95% C.I. = [0.92, 2.98]). **(E)** Data in **B** normalized to 20 min (n = 15 mice; one-way ANOVA main effect of paradigm type, $F(2,42) = 55.75$, $P = 1.5e^{-12}$; Tukey HSD multiple comparisons, 2hr vs. 4hr: P = 0.59, 95% C.I. = [-0.19, 0.46]; 2hr vs. HFD, $P = 2.4e^{-10}$, 95% C.I. = [-1.4877,-0.83311]; 4hr vs. HFD, $P = 1.1e^{-11}$, 95% C.I. = [-1.62,-0.97]). **(F)** Head-fixed ethanol consumption in 2-cycle paradigm sorted by sex (n = 9 male and 6 female mice; unpaired *t*-test, $t(13) = -3.5834$, P = 0.003). **(G)** Data in **D** normalized to 20 min (n = 15 mice; one-way ANOVA main effect of paradigm type, $F(2,42) = 75.8$; $P = 1.2e^{-14}$; Tukey HSD multiple comparisons, 2hr vs. 4hr: p = 0.78, 95% C.I. = [-0.31, 0.56]; 2hr vs. HFD: $P = 1.4e^{-12}$, 95% C.I. = [-2.28, −1.41]; 4hr vs. HFD: $P = 1.9e^{-13}$, 95% C.I. = [2.40, −1.53]). **(H)** Consumption in the 1-cycle paradigm sorted by sex (n = 4 male and 11 female mice; unpaired *t*-test, $t(13) = -2.58$, P = 0.023). **(I)** Across animal consumption variability. Coefficient of variation calculated across mice for mean consumption on 2-h sessions of week 2 DID. For head-fixed drinking, it was calculated across mean head-fixed consumption over the first 3 days of HFD (Levene's test, P = 0.19). **(J)** Across session consumption variability. Coefficient of variation calculated for each mouse across 2-h sessions during week 2 of DID and across first 3 head-fixed drinking sessions (n = 15 mice; unpaired *t*-test, $t(14) = -1.81$, P = 0.092). **(K)** Same as I but for the 1-cycle paradigm (Levene's test, P = 0.99). **(L)** Same as J but for 1-cycle paradigm (n = 15 mice; unpaired *t*-test, $t(14) = -0.22$, P = 0.83). Significance denoted as *p < 0.05; **p < 0.01; ***p < 0.005. All error bars are standard error of the mean.

3.3. *Temporal dynamics of ethanol consumption during head-fixed drinking*

Our analyses thus far show similarities between DID and HFD for sex-dependent drinking and consumption variability. In our paradigm, mice self-pace ethanol delivery by licking the spout to trigger additional drops separated by pseudorandom delay. We analyzed the temporal dynamics of drinking pattern in HFD sessions to evaluate whether head-fixed mice show more engagement with triggering ethanol drops in the first drinking block compared to the second drinking block. We quantified the proportion of total drops that were dispensed in 2-min bins across 20 min of drinking (Fig. 3A and B). For both 2-cycle and 1-cycle groups, mice triggered more ethanol deliveries during the first 10 min of the session compared to the last 10 min (Fig. 3C and D). We computed an early engagement score by normalizing the number of drops delivered in the first 10 min by deliveries in the last 10 min. There was no relationship between the early engagement score and the amount of ethanol consumed during HFD (Fig. 3E and F). These results show that head-fixed mice exhibit early engagement with ethanol. Due to limitations with our paradigm (see section 4.5), it is currently difficult to assess the relationship between early ethanol engagement and frontloading behavior previously described in home cage and operant drinking tasks (Ardinger et al., 2022).

3.4. *Licking dynamics during head-fixed ethanol consumption*

Given the similar level of consumption observed in the two groups of HFD mice, we focused our remaining analysis on mice in the 1-cycle

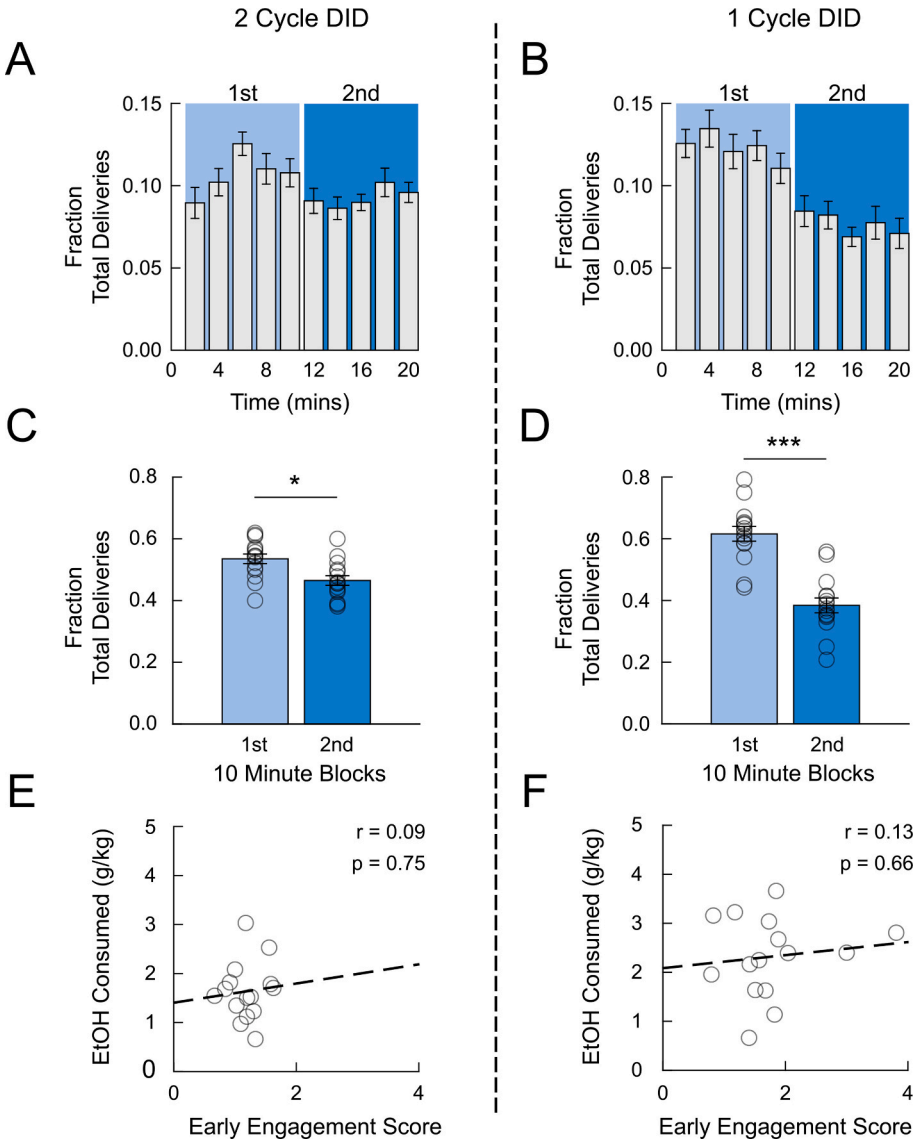

Fig. 3. Temporal dynamics of ethanol consumption during head-fixed drinking. (A, B) Fraction of ethanol drops delivered in 2-min bins across 1st and 2nd 10 min drinking blocks of head-fixed drinking in the 2-cycle (A) and 1-cycle (B) paradigms. **(C)** Comparison of ethanol consumption during early (1st 10 min) and late (2nd 10 min) drinking blocks (n = 15 mice; paired *t*-test, t(14) = 2.25, P = 0.041). **(D)** Same as (C) but for the 1-cycle paradigm (n = 15 mice; paired *t*-test, t(14) = 4.83, P = $2.7e^{-4}$). **(E, F)** Pearson's correlation of early engagement score against head-fixed consumption for 2-cycle (E) and 1-cycle (F) DID paradigms. Significance denoted as *p < 0.05; **p < 0.01; ***p < 0.005. All error bars are standard error of the mean.

cohort. The HFD paradigm allows high temporal resolution tracking of licking behavior. We analyzed licking dynamics to better understand ethanol consumption behavior during head-fixation. Surprisingly, we observed licking during the pre-drinking period even when no ethanol was available for consumption, although there was significantly more licking during the drinking period (Fig. 4A–C). This pre-drinking licking is unlikely to reflect the motivation to consume ethanol as there was no relationship between the pre-drinking licking frequency and the number of ethanol drops delivered in the subsequent drinking session (Fig. 4D). Expectedly, the licking frequency during the drinking period was correlated with drop delivery (Fig. 4E), demonstrating that mice modulate their licking to acquire varying levels of ethanol during HFD.

Next, we analyzed how licking behavior evolves as a function of time during HFD sessions. The lick rate decreased in the second 10 min of drinking compared to the first 10 min (Fig. 4F). To investigate this further, we aligned licks to the time of individual ethanol deliveries and tracked across the session the number of licks elicited within a 5s window after each delivery. Average licks per drop decreased steadily over the course of the 20 min drinking session (Fig. 4G). Inspection of individual licking traces showed that some drop deliveries were not immediately followed by licking (Fig. 4A and B). The fraction of deliveries with licks within a 5s window also decreased across the session (Fig. 4H). However, the mean latency to first lick after reward delivery did not change across the session (Fig. 4I). Taken together with the previous early engagement analyses (Fig. 3), these results show that mice trigger more drop deliveries and elicit more vigorous licking responses earlier in the drinking session.

3.5. *Comparing head-fixed ethanol and sucrose consumption*

We tested whether mice with *ad libitum* water and food access (i.e., non-deprived) voluntarily consume sucrose during head-fixation. We reasoned that this would accomplish two goals: 1) it would allow us to compare head-fixed ethanol consumption to consumption of another rewarding liquid; and 2) it would allow future head-fixed studies to determine if neural correlates of consumption are specific for ethanol.

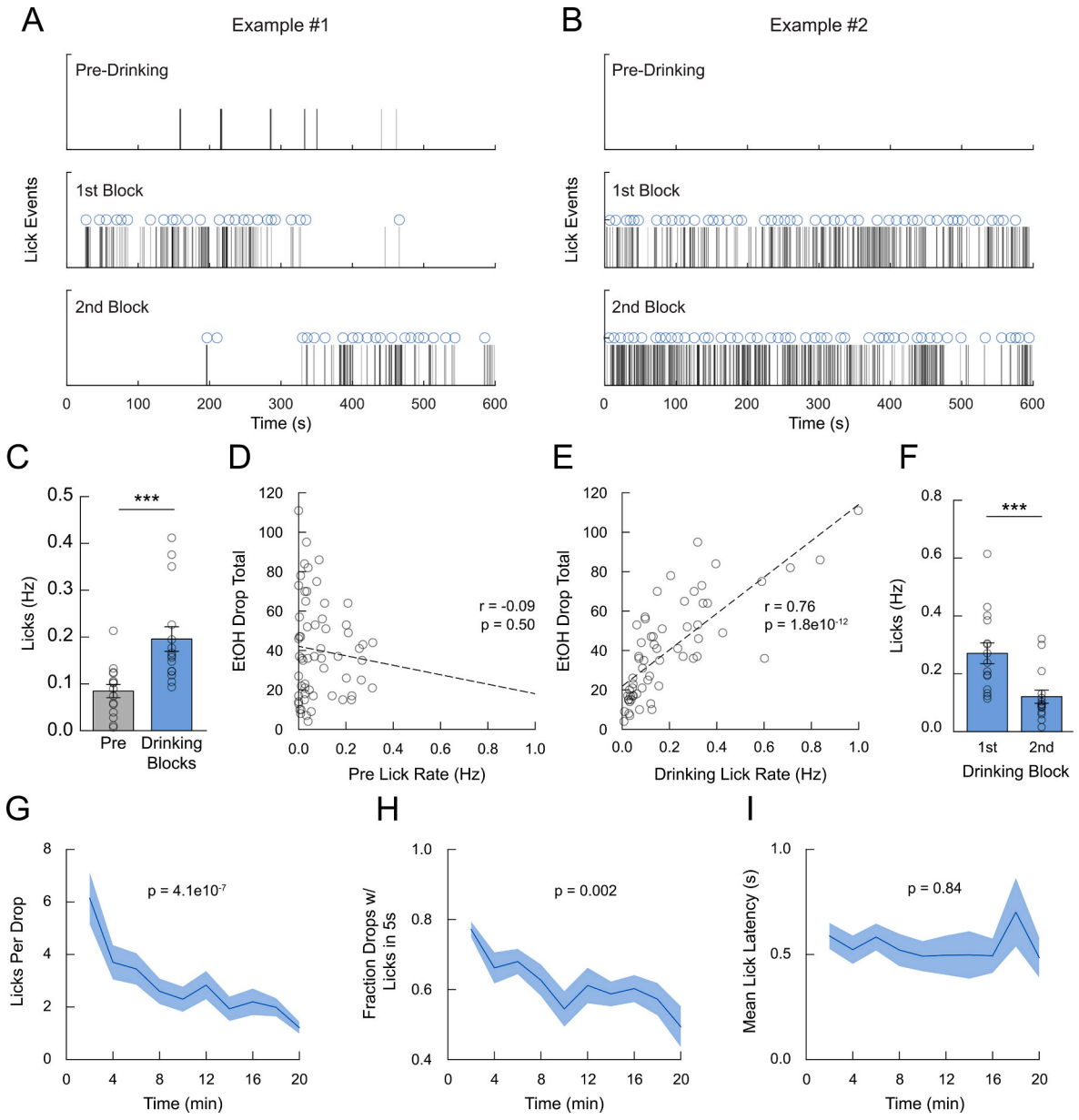

Fig. 4. Licking dynamics during head-fixed ethanol consumption. **(A, B)** Licking activity on two example head-fixed drinking days. **(C)** Comparison of licking frequency during pre-drinking baseline period and during drinking (n = 15 mice; paired *t*-test, t(14) = −3.18, P = 0.007). **(D)** Correlation of pre-drinking licking frequency against total number of ethanol drops delivered for each HFD day (n = 60 sessions from 15 mice). **(E)** Correlation of drinking lick rate and number of delivered drops (n = 60 sessions from 15 mice). **(F)** Mean licking activity during 1st and 2nd 10-min drinking sessions (n = 15 mice; paired *t*-test, t(14) = 5.02, P = $2.0e^{-4}$). **(G)** Mean number of licks in a 5s window for each ethanol delivery across 20 min of drinking in 2-min intervals (n = 15 mice; one-way ANOVA main effect of time, F(9,140) = 6.02, P = 4.1e-07). **(H)** Fraction of delivered drops with mice licking within a 5s window (n = 15 mice; one-way ANOVA main effect of time, F (9,140) = 3.11, P = 0.002). **(I)** Mean latency to lick after ethanol drop delivery across drinking (n = 15 mice; one-way ANOVA main effect of time, F(9,139) = 0.54, P = 0.85). Significance denoted as *p < 0.05; **p < 0.01; ***p < 0.005. All error bars and shading are standard error of the mean.

Mice in the 1-cycle group were given a four-day break after their last ethanol/quinine head-fixed drinking session. Following this break, head-fixed mice self-administered 3% sucrose (w/v) during head-fixation with the same procedure used for ethanol consumption (Fig. 5A).

We found that head-fixed mice readily consumed sucrose. Unlike for ethanol, sucrose consumption did not decrease across the 20-min session and there was no difference in the number of delivered drops or the licking rate between the first and last 10 min of drinking (Fig. 3A–D, 4F, 4G, and 5B-D). Although the number of licks per delivered drop of sucrose appeared to decrease across the drinking session (Fig. 5E) similar to ethanol (Fig. 4G), this effect was not statistically significant. Moreover, in contrast to ethanol (Fig. 4H), the proportion of drops with licking within 5s after delivery was similar across the session (Fig. 5F).

We directly compared ethanol and sucrose HFD data to further evaluate differences and similarities in the consumption of these liquids. Across mice, there was no relationship between the amount of ethanol and sucrose consumption (Fig. 5G). On average, mice delivered the same number of ethanol and sucrose drops (Fig. 5H) but showed less early engagement for sucrose than for ethanol (Fig. 5I). Comparison of licking behavior showed similar licking rates in the pre-drinking and drinking session for ethanol and sucrose (Fig. 5J). Examining licking behavior aligned to the time of ethanol or sucrose delivery showed similar licking dynamics and rates for the two liquids (Fig. 5K and L). Together these analyses suggest that consumption and licking correlates of early engagement are more pronounced for ethanol than sucrose HFD.

3.6. Two-photon calcium imaging of the anterior cingulate cortex during head-fixed ethanol drinking

The prefrontal cortex is a key brain structure for high-level cognitive functions like attention, decision-making, and sensorimotor control. Acute ethanol intoxication is associated with deficits in these same functions, suggesting that drinking may affect prefrontal cortical activity. Previous *ex vivo* electrophysiological studies show that ethanol modulates a multitude of intrinsic electrophysiological and synaptic properties of neurons (Harrison et al., 2017; McCool, 2011). However,

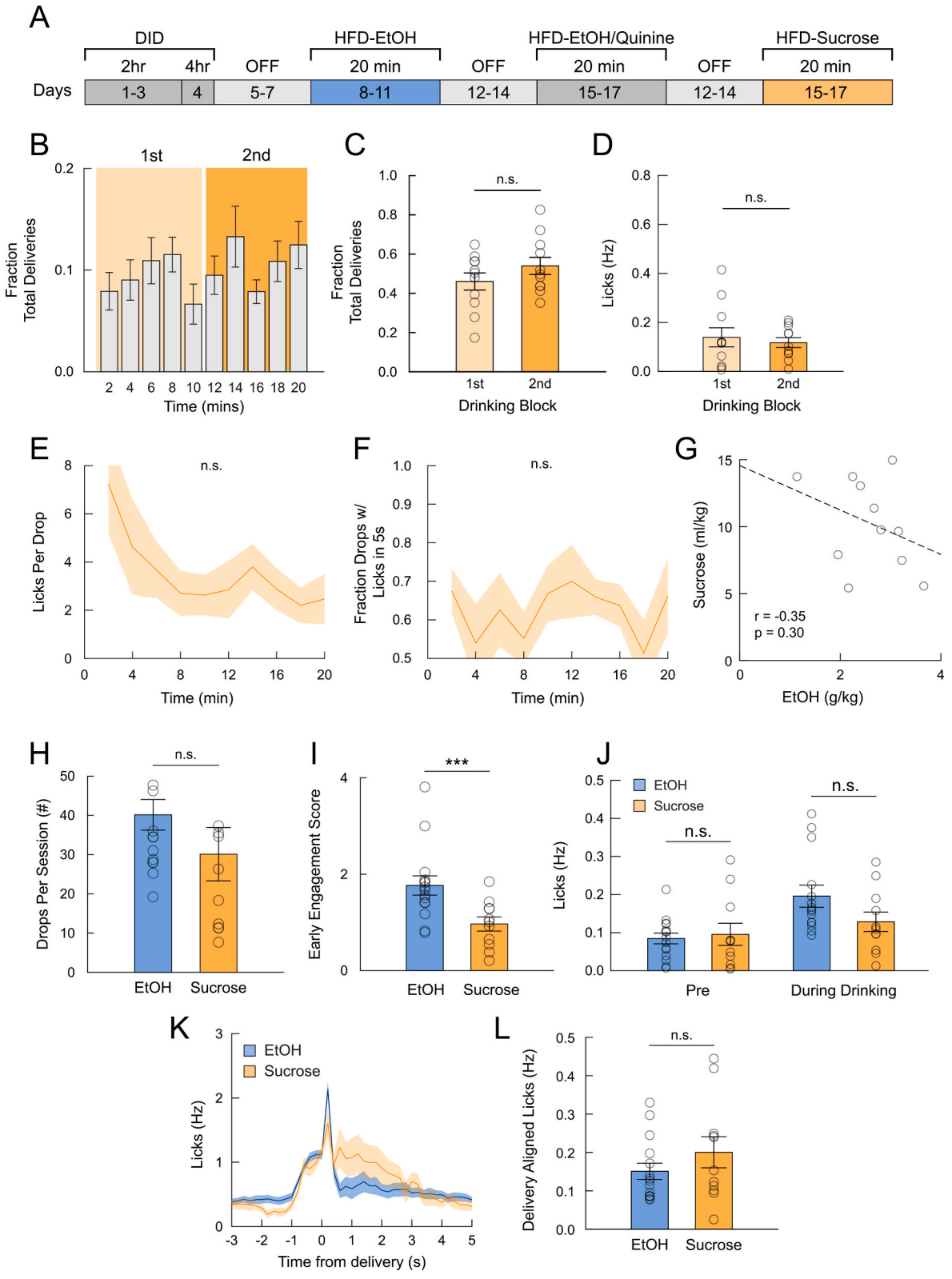

(caption on next page)

Fig. 5. Comparison of ethanol and sucrose consumption during head-fixed drinking. (A) Timeline for experiments. **(B)** Fraction of deliveries across time during head-fixed sucrose consumption. **(C)** Comparison of sucrose deliveries triggered in 1st and 2nd sucrose drinking sessions. (n = 11 mice; paired *t*-test, t(10) = −0.91, P = 0.38). **(D)** Comparison of lick rates in 1st and 2nd sucrose drinking sessions (n = 11 mice; paired *t*-test, t(10) = 0.62, P = 0.55). **(E)** Mean number of licks in a 5s window for each sucrose delivery across 20 min of drinking in 2-min intervals (n = 11 mice; one-way ANOVA main effect of time, F(9,87) = 1.33, P = 0.23). **(F)** Fraction of sucrose deliveries with a lick within 5s after delivery (n = 11 mice; one-way ANOVA main effect of time, F(9,87) = 0.64, P = 0.76). **(G)** Correlation of head-fixed ethanol and sucrose consumption. **(H)** Comparison of ethanol and sucrose drops delivered during head-fixed consumption (n = 15 and 11 mice for ethanol and sucrose, respectively; two-sample *t*-test, t(24) = 1.36, P = 0.19). **(I)** Early engagement score for ethanol and sucrose consumption (n = 15 and 11 mice for ethanol and sucrose, respectively; t(24) = 3.01, P = 0.006). **(J)** Comparison between ethanol and sucrose for pre-drinking and drinking licking rates (n = 15 and 11 mice for ethanol and sucrose, respectively; two-way ANOVA main effect of drink type, F(1,48) = 1.38, P = 0.25; main effect of session type, F(1,48) = 8.99, P = 0.0043; interaction between drink and session type, F(1,48) = 2.67, P = 0.11′ multiple comparisons with Tukey HSD, ethanol-pre vs. sucrose-pre: 95% C.I. = [-0.08 0.10], P = 0.99; ethanol-drinking vs. sucrose drinking: 95% C.I. = [-0.16 0.02], P = 0.21. **(K)** Licking dynamics for ethanol and sucrose head-fixed consumption aligned to delivery. **(L)** Comparison of mean licking rate in a 3s window after sucrose and ethanol delivery (n = 15 and 11 for ethanol and sucrose; two-sample *t*-test, t(24) = −1.17, P = 0.25).

there is a paucity of data on how acute ethanol consumption affects the *in vivo* activity of prefrontal cortical networks during voluntary consumption. Our predominant goal in establishing a head-fixed ethanol consumption paradigm is to enable real-time interrogation of neural circuit function across acute and repeated ethanol consumption and during other ethanol-related behaviors. As an example application of our paradigm, we combined head-fixed drinking with two-photon calcium imaging to determine how ethanol consumption affects the activity of single prefrontal cortical neurons and network level interactions between neurons. Importantly, head-fixed mice consumed ethanol during two-photon imaging, achieving binge-like BEC levels (199.3 ± 62.19 mg/dL, n = 4 mice).

3.7. Effect of acute ethanol consumption on tonic activity of single ACC neurons

We used a transgenic mouse line (CaMKII-Cre x Ai148D on a C57/BL6 background) that targets GCaMP6f expression to excitatory pyramidal neurons in the cortex. Mice were implanted with a chronic window over the midline in the frontal cortex. We targeted recordings in the anterior cingulate cortex (ACC), a subdivision of the mouse prefrontal cortex that is accessible for two-photon imaging without brain lesioning optical implants (Fig. 6A–C). Although we could longitudinally track individual neurons across days, here we prioritized studying the effect of acute ethanol on large neuronal populations and analyzed the activity of >1200 recorded cells (n = 1250 neurons). Calcium events were detected from GCaMP6f fluorescence traces to quantify event frequency and amplitude. Inspecting the activity of individual neurons during pre-drinking and drinking showed heterogeneous effects of ethanol consumption on single neuron activity. The simultaneously recorded example neurons shown in Fig. 6D illustrate 3 types of observed responses over the time course of the entire drinking session: an increase, decrease, or no change in neuronal activity.

To assess the population-level effect of ethanol on ACC activity, we compared the event rate of calcium transients during the pre-drinking and drinking periods. There was no change in activity levels when

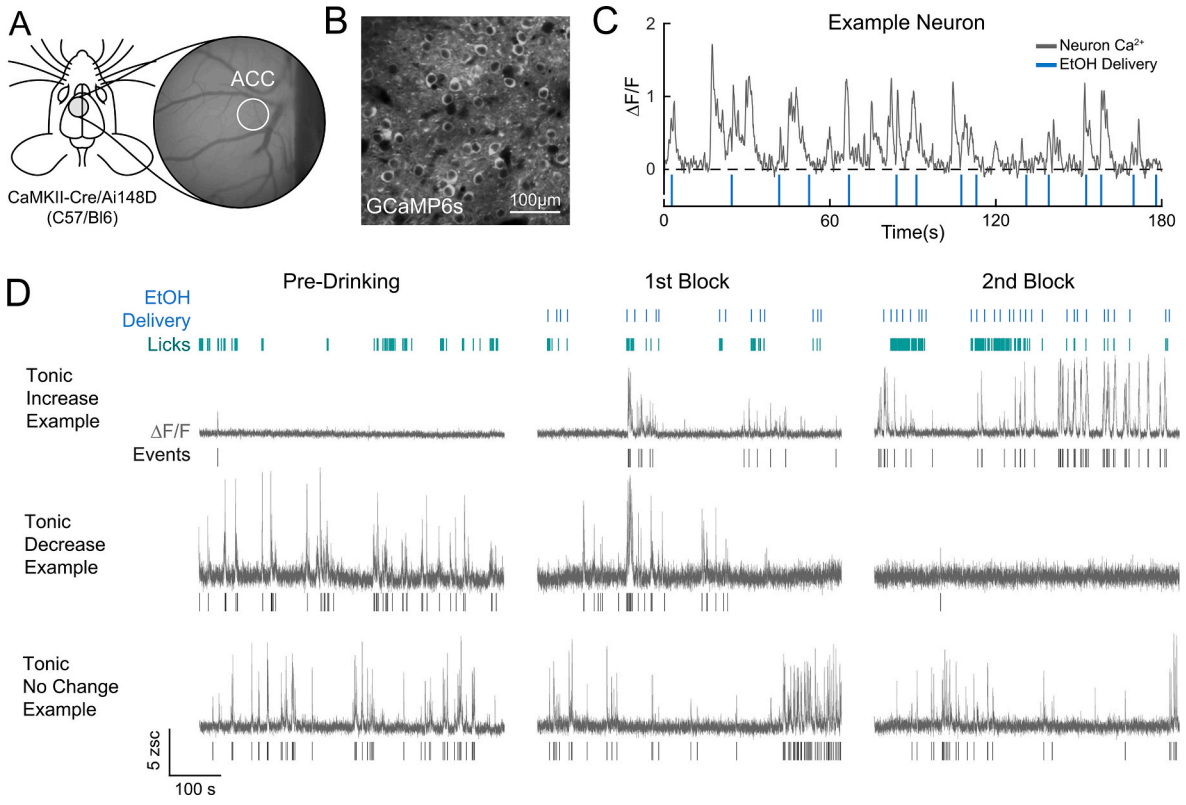

Fig. 6. Two-photon calcium imaging of anterior cingulate cortex (ACC) activity during head-fixed ethanol consumption. (A) Chronic window implant site in the frontal cortex of transgenic mice expressing GCaMP6f in excitatory pyramidal neurons. **(B)** GCaMP-expressing ACC neurons. **(C)** Activity of an example neuron along with ethanol delivery times. **(D)** Three simultaneously recorded example neurons (rows) showing tonic increase, decrease, or no change in activity from pre-drinking to the later drinking sessions. Top rows show licking behavior (green) and ethanol delivery (blue).

considering all recorded neurons (Fig. 7A and B). This lack of a population level effect could be driven by heterogeneity in the response profiles of individual neurons, as suggested by the single neuron examples (Fig. 6D). We used a shuffle test to identify neurons with increased or decreased activity during drinking as compared to the pre-drinking period. We circularly permuted each neuron's activity to randomize the timing of calcium events while preserving the temporal structure of activity (see **Methods** for details). Comparing the observed activity difference in pre-drinking and drinking periods with the shuffled data showed that alcohol increased and decreased the activity of a similar proportion of neurons; the activity of 11.8% of neurons was increased and the activity of 13.4% of neurons was decreased. These cells showed significantly increased or decreased activity in the last 2nd drinking block compared to the pre-drinking period (Fig. 7C–F). Given that ethanol consumption had a persistent effect on the activity of these cells, we refer to them as tonically modulated neurons. Surprisingly, despite ethanol's effect on many intrinsic neuronal properties and on synaptic transmission, *in vivo* activity rates for the majority of ACC neurons are remarkably resilient against large changes with binge-like levels of ethanol consumption.

3.8. Mean population activity tracks ethanol deliveries

In the above analysis, we assessed the influence of ethanol by comparing activity levels between the pre-drinking and the drinking period. A potential caveat is that pre-drinking activity reflects not only the baseline activity of neurons but also additional factors like expectation for alcohol which may be different during the pre-drinking and drinking periods. To address this concern, we restricted our analysis to only the drinking period to determine how ACC activity is modulated as a function of ethanol drop delivery. For each recording session, we determined in 2-min bins the mean session activity (i.e., the mean event rate of all simultaneously recorded neurons) and the fraction of total ethanol drops delivered across the drinking period (Fig. 8A). Population ACC activity seemed to track ethanol deliveries. There was a positive correlation between the fraction of ethanol drops delivered and mean session activity (Fig. 8B), but no such relationship was observed between time shuffled mean session activity and drop delivery ($r = -0.53$, $p > 0.05$). Performing the same analysis at a single neuron level revealed only a small fraction of neurons with a significant positive correlation (4.6%), suggesting that population-level activity may better reflect ethanol deliveries over the time scale of minutes.

Mice consume most ethanol drops within a short time window after delivery (Fig. 4H). Indeed, 68.6 ± 2.2% of all licks occurred within 10s of ethanol deliveries (n = 11 sessions). We excluded neuronal activity during this consummatory period and recomputed the correlation between population activity and number of ethanol drops in 2-min bins. A significant correlation remained between activity and ethanol deliveries (Supp. Figs. 2A and B). Moreover, we did not detect a significant correlation between mean session activity and lick rate in 2-min bins (Supp. Figs. 2C and D). These results suggest that consummatory processes (like licking) alone cannot explain the correlation between ACC activity and number of ethanol deliveries.

To better interpret the activity of tonically modulated neurons (Fig. 7), we analyzed the relationship between ethanol deliveries and the activity of tonic neurons, determined as the mean event rate of significantly modulated neurons within individual sessions (Supp. Fig. 3). In contrast to the overall ACC population, the activity of tonic neurons seemed to track ethanol deliveries only during the earlier part of the drinking session, showing increased or decreased activity at the end that

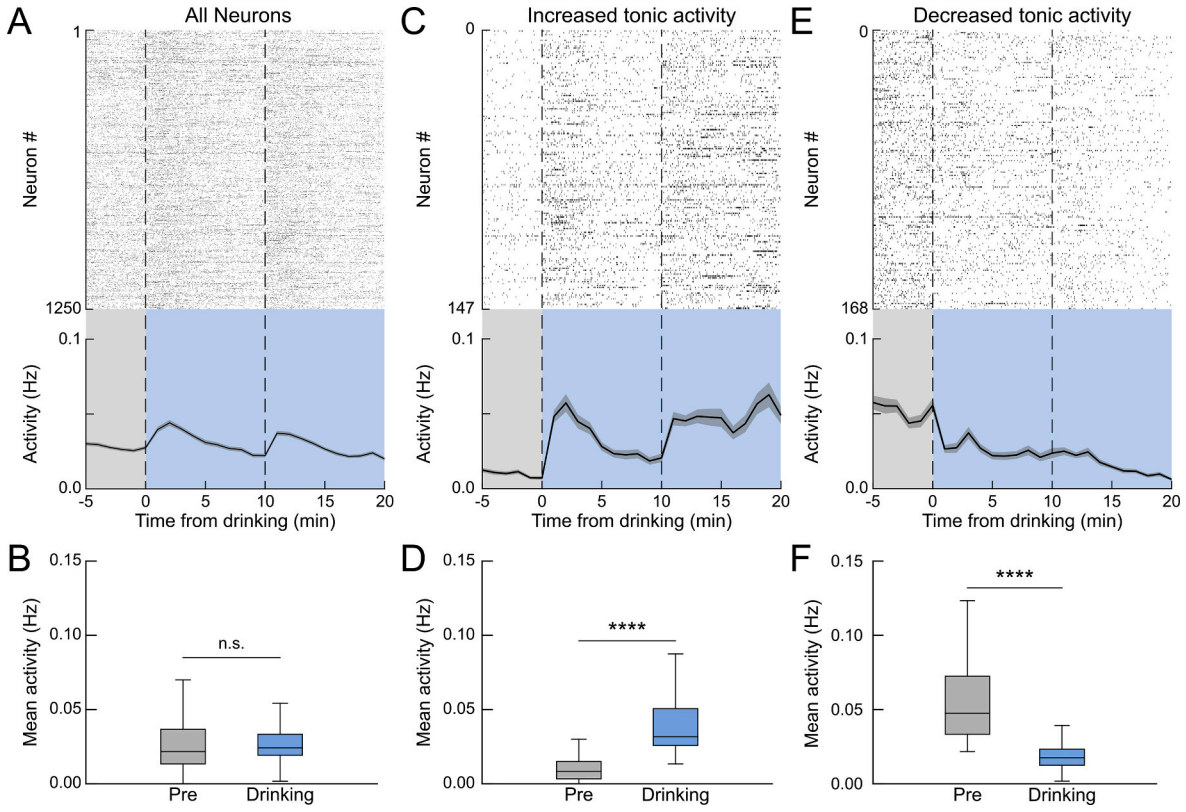

Fig. 7. Effect of ethanol consumption on tonic activity of single ACC neurons. (A) Raster plot (top) showing detected calcium events for all individual neurons across the pre-drinking and drinking blocks (delineated by dashed lines and shading) and population mean even rates (bottom) in 1 min bins (bottom, shading is SEM). **(B)** Mean event rate averaged across pre-drinking (gray) and 2nd drinking block (blue) for all neurons (paired *t*-test, $t(2498) = -0.0023$, $P = 1.0$; n = 1250 neurons) **(C,D)** Same as **A,B**, except for neurons with increased tonic activity (paired *t*-test, $t(292) = -14.2$, ****$P < 10^{-34}$; n = 147 neurons). **(E,F)** Same as **A,B** except for neurons with decreased activity (paired *t*-test, $t(334) = 14.0$, ****$P < 10^{-34}$; n = 168 neurons).

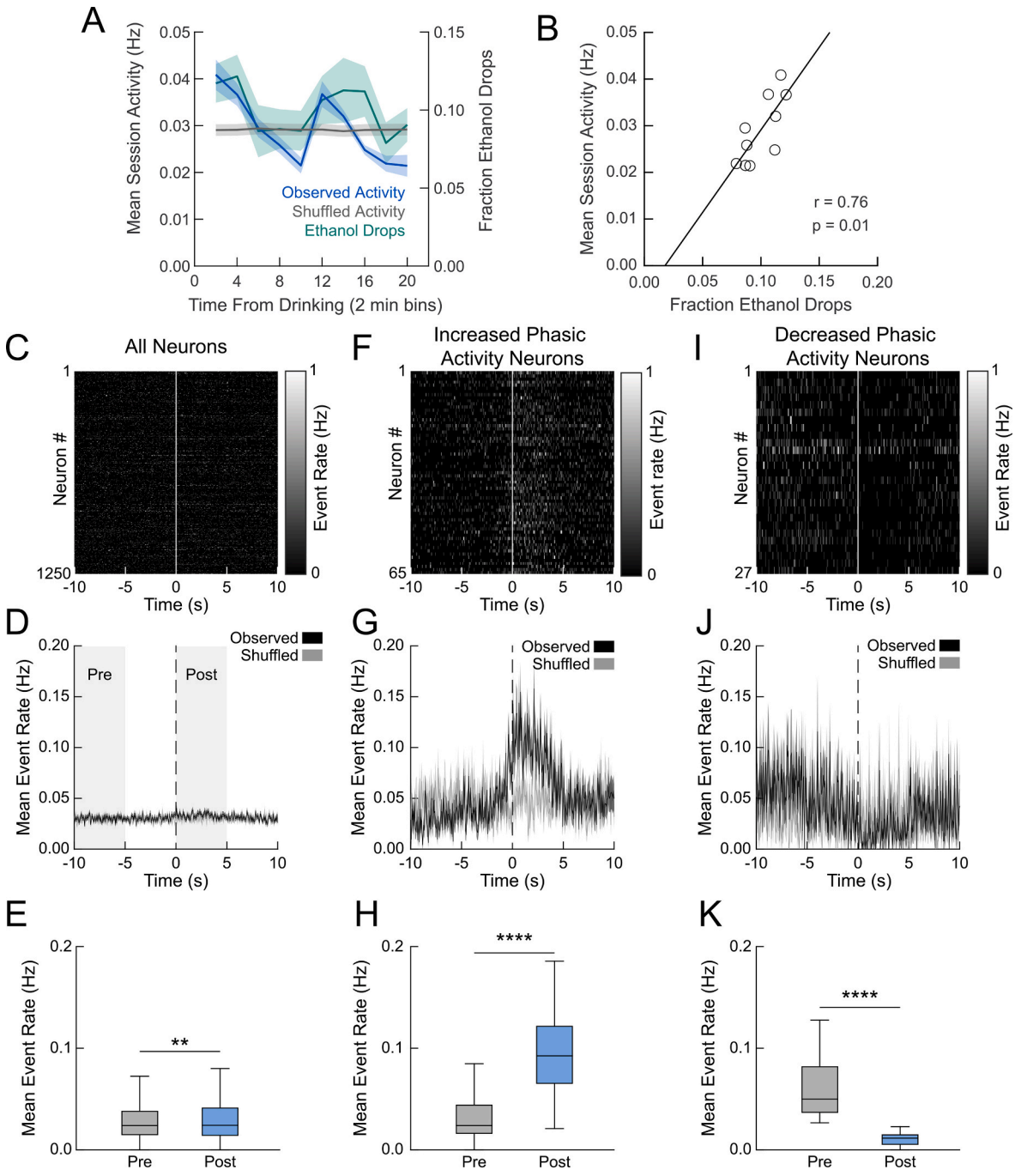

Fig. 8. Effect of ethanol consumption on mean session activity and single neuron responses. (A) Mean activity of all simultaneously recorded neurons (blue) plotted across 20 min of drinking in 2 min bins and compared to shuffled activity (gray) and fraction of ethanol drops delivered (green). **(B)** The mean session activity rate plotted against the fraction of ethanol deliveries in each 2-min bin in **A** (n = 12 sessions from 4 mice). **(C)** Colormap plot of activity rate for all neurons aligned to the first lick after ethanol delivery. **(D)** Average activity (black) of all neurons aligned to first lick following ethanol delivery compared to shuffled activity (light gray). Gray shadings show window for calculating pre and post activity in E, H, and K. **(E)** Activity over a 5s window averaged before (pre) and after (post) first lick following ethanol delivery (paired *t*-test, t(2498) = −2.88, *P = 0.004; n = 1250 neurons). **(F–H)** Same as C-E, except for the neurons with increased phasic activity (paired *t*-test, t(128) = −11.5, ****P < 10^{-20}, n = 65 neurons) **(I–K)** Same as C-E, except for neurons with decreased phasic activity (paired *t*-test, t(52) = 5.29, ****P = 0.000002; n = 27 neurons).

deviated from the ethanol delivery rate (Supp. Figs. 3A and C). As a result, there was not a significant correlation between ethanol deliveries and mean session tonic activity when considering the entire 20-min drinking period (Supp. Figs. 3B and D). These findings suggest that as a population these neurons reflect the tonic effect of ethanol with a delay, as would be expected for the intoxicating effects of ethanol.

3.9. Subset of single neurons are phasically modulated around ethanol deliveries

The above analyses consider activity changes during drinking on the timescale of the entire drinking session or minutes, possibly reflecting the cumulative effect of ethanol consumption. Next, we analyzed single neuron responses aligned to the time of first lick after individual ethanol deliveries (Fig. 8C). We identified phasically modulated neurons by

statistically comparing activity after delivery to a preceding baseline period (gray shadings in Fig. 8D). When considering the whole recorded population, there was no significant change in activity following single ethanol deliveries. Of all recorded neurons, 5.2% showed phasic activation after ethanol delivery while 2.2% of neurons were inhibited (Fig. 8F–K). Importantly, time shuffled neuronal activity was not modulated around ethanol deliveries for these neurons (Fig. 8G,J). Hence, a small subset of ACC neurons show phasic responses around ethanol deliveries, possibly reflecting ethanol receipt and/or consumption-related processes.

We also determined the overlap in neurons with tonic activity modulation and neurons showing delivery-aligned phasic responses (Supp. Fig. 4). Overall, 30.7% of all recorded ACC neurons showed significant tonic or phasic modulation in their activity. A great majority (94%) showed exclusive tonic or phasic modulation (Supp. Fig. 4A). In agreement, the time-aligned responses of tonic neurons showed little phasic modulation around ethanol deliveries (Supp. Figs. 4B and C). Similarly, there was no difference in pre-drinking and drinking activity of phasically modulated neurons (Supp. Figs. 4D and E). These analyses suggest that tonic and phasic effects of ethanol are reflected in largely separate subpopulations of ACC neurons.

3.10. Effect of ethanol consumption on pairwise between-neuron correlations

The above analyses show that acute ethanol consumption modulates the activity of a subset of ACC excitatory neurons over slow (minutes) and fast (seconds) time scales. Information processing in cortical

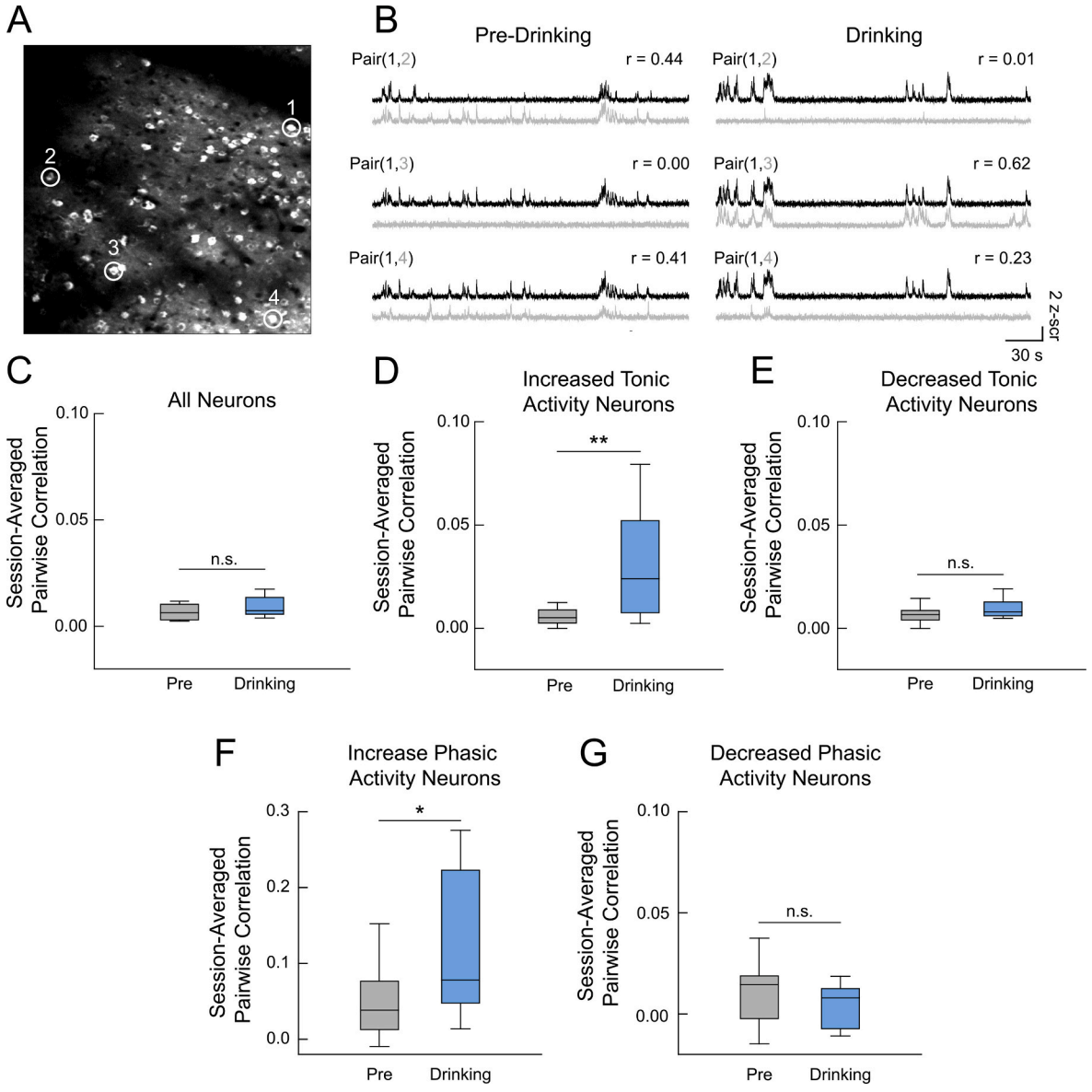

Fig. 9. Effect of ethanol consumption on pairwise activity correlations between neurons. (A) Example field of view showing the spatial location of four representative neurons (white circles/numbers). **(B)** Representative activity of pairs of neurons shown in (A) for pre-drinking and the 2nd drinking blocks. **(C)** Mean pairwise correlation coefficients averaged for all simultaneously recorded unique neuronal pairs during last 5 min of pre-drinking and drinking blocks (paired *t*-test, t(20) = −1.55, P = 0.14; n = 11 sessions). **(D)** Same as C, except for pairwise correlations between neurons with increased tonic activity (paired *t*-test, t(20) = −3.12, **P = 0.005; n = 11 sessions). **(E)** Same as C, except for decreased tonic activity neurons (paired *t*-test, t(20) = −0.24, P = 0.81; n = 11 sessions). **(F)** Same as C, except for neurons with increased phasic activity (paired *t*-test, t(18) = −2.11, *P = 0.049; n = 10 sessions). **(G)** Same as C, except for neurons with decreased phasic activity (paired *t*-test, t(12) = 0.93, P = 0.37; n = 7 sessions). Note that for **D-G,** at least 2 significantly modulated neurons are required for the session to be included in the analysis.

networks is shaped by correlated activity between neurons in addition to single neuron activity levels (Cohen and Kohn, 2011; Kohn et al., 2016). We took advantage of the large number of simultaneously recorded neurons in our dataset to test the effect of ethanol consumption on between-neuron correlations. For each recording session, we computed the Pearson correlation coefficient between the activity of unique pairs of neurons (Fig. 9A and B). Visualizing the activity of single example pairs showed diverse changes, with correlations increasing, decreasing, or being unaffected during the end of the drinking session (last 5 min of the second drinking block) compared to pre drinking (Fig. 9B). To examine this process at the population level, we compared correlations averaged over all unique pairs of neurons recorded simultaneously in single behavioral sessions. The pairwise correlation was similar during drinking and pre-drinking periods (Fig. 9C). Alcohol receipt and/or consummatory licking during the drinking period did not exert a detectable effect as pairwise correlations during the pre-drinking and drinking periods were similar when neuronal activity 10s after ethanol deliveries was excluded (Supp. Fig. 5A).

Next, we examined how alcohol affects pairwise correlations for subgroups of neurons showing activity modulation during drinking. The correlation between neurons with increased tonic activity was higher during drinking than during pre-drinking (Fig. 9D). This effect was also observed when activity after ethanol deliveries was excluded from the analysis (Supp. Fig. 5B). In contrast, for neurons with increased phasic activity, drinking correlation was higher than pre-drinking only when neuronal activity during ethanol deliveries was included in the analysis (Fig. 9F; Supp. Fig. 5D). Neurons with decreased tonic or phasic activity modulations did not show significant changes in pairwise correlations with drinking (Fig. 9E,G; Supp. Figs. 5C and E). These results suggest that acute ethanol intoxication increases activity synchrony in a subset of ACC neurons.

4. Discussion

4.1. Voluntary alcohol drinking in head-fixed mice

Neuroscientific research has benefitted from the rapid development of technologies to measure and manipulate neuronal and non-neuronal circuits. The rise of multiphoton imaging, high-density electrophysiological electrodes, fluorescence-based voltage sensors, and variety of other techniques have provided new insights into the spatiotemporal dynamics of neuronal computations important for behavioral control (Ji et al., 2016; Liu et al., 2022; Steinmetz et al., 2018; Tian et al., 2023). However, many of these tools currently require immobilization of the animal's head. This methodological limitation necessitates the adaptation of current freely moving behavioral paradigms to head-fixed counterparts.

Here, we demonstrate the feasibility of a 'head-fixed drinking' (HFD) variant of the well-characterized 'drinking-in-the-dark' (DID) model of binge-like ethanol consumption. In our animal cohorts, mice consumed ~1.5–2 g/kg of 20% ethanol over the course of 20 min, which represents an average rate of ~0.1 g/kg/min. Comparatively, mice undergoing the traditional DID paradigm consume ~3–4 g/kg over 2 h, which corresponds to a rate of ~0.025 g/kg/min (Thiele and Navarro, 2014). Therefore, although the overall ethanol volume consumed in HFD is less than DID, the rate is higher, resulting in pharmacologically relevant BEC levels for studying binge-like consumption. Given the rapid rate of ethanol consumption during head-fixation, this paradigm is a potential model for high-intensity binge drinking (Patrick and Azar, 2018), although further work is required to explore this possibility.

Despite the difference in intake rate, we found several similarities between home cage and head-fixed drinking. First, female mice consumed more ethanol during HFD than males, which is consistent with home cage drinking (Fig. 2F, H). This suggests that factors driving sex-differences in ethanol consumption behavior remain in effect with head-fixation. Second, session-to-session and animal-to-animal variability was similar between home cage DID and HFD drinking (Fig. 2I-L).

4.2. Advantages of head-fixed behavior

Head-fixation benefits several other detailed measurements of animal behavior (Ozgur et al., 2023). For example, using high resolution cameras, licking kinetics and microstructures can be readily recorded. Additionally, facial movements, whisking, and pupil diameter can be quantified using open-source, machine learning algorithms such as DeepLabCut (Nath et al., 2019). Head-fixation also allows for more controlled sensory environments that range in complexity from precise auditory and visual stimulation such as used for operant responding to closed-loop virtual reality environments. Controlling the sensory environment reduces trial-to-trial variability in contextual learning, operant conditioning, and sensorimotor decision-making. These behaviors (and others) have all been applied in the alcohol research field, but not within the head-fixed domain. Therefore, adapting these behavioral paradigms to head-fixed drinking will serve as a useful complementary approach to the freely moving counterparts and will allow application of recording modalities like two-photon imaging for assessment of circuit mechanisms.

Even though there are limitations to head-fixed behavior (discussed below), several other natural and drug reward paradigms have been adapted for head-fixed mice including go/no-go tasks, Pavlovian conditioning, sensorimotor decision making and operant natural reward/drug reward self-administration (Bloem et al., 2017; Breton-Provencher et al., 2022; Gordon-Fennell et al., 2023; Huda et al., 2020; Ottenheimer et al., 2023; Vollmer et al., 2021 ;Vollmer et al., 2022). These tasks model processes like reward learning, motivation, expectation, attention, and others that play important roles in alcohol-related behaviors. By demonstrating voluntary alcohol drinking in head-fixed mice, this study lays the groundwork for adapting these more sophisticated head-fixed paradigms for alcohol studies.

4.3. Important considerations for head-fixed drinking

A critical consideration for implementing HFD is the precise positioning of the lick spout. It is recommended that a high-resolution fixed camera be used to record the relative positioning of the lick spout with each individual mouse. This reduces the variability in drinking due to unfamiliar lick spout placement. In addition, ethanol spillage, that is drops of alcohol triggered by licking but not consumed, can be a factor in drinking heterogeneity. The use of a high-resolution camera can help identify drops being delivered but not consumed. We placed a weigh boat underneath the spout to quantify unconsumed ethanol and found that spillage does occur but relatively infrequently. This also helps calibrate the solenoid delivery of ethanol by using both a volume release (measured by the graduated syringe containing the ethanol reservoir), the weight of the ethanol that lands on the weigh boat, the duration of time the solenoid was open (to deliver a single drop), and the total number of drops. A calibration table should be generated by varying the number of drops and the time the solenoid is open and interpolating a curve to the total delivery. Importantly, the BEC should be plotted against the measured consumption at least in a subset of animals or sessions to infer the relationship between consumption and BEC.

4.4. General limitations of head-fixed behavior

Though head-fixation provides several benefits for some quantitative measures, it also presents a few general experimental limitations. First, HFD requires the surgical implantation of a head-plate for head-immobilization. Custom stainless-steel head-plates can be manufactured relatively cheaply from open-source designs and can be recovered and sterilized for reuse across animals. Multiple surgical procedures for affixing the headplate to the animal's skull have been published with the

most common method being the use of dental cement (Carlsen et al., 2022; Holtmaat et al., 2012; Manita et al., 2022). Though headplate attachment is a relatively simple procedure, it does require substantial recovery by the animal especially if combined with a cranial window implant.

Second, HFD requires a platform with head-fixation bars that allows the animal to be supported while the head is immobilized. Custom head-fixation rigs can be built using readily available parts from opto-mechanical suppliers (e.g., Thor Labs) (Huda et al., 2020; Lee et al., 2022; O'Connor et al., 2010; Ozgur et al., 2023). The precise configuration will depend on the experimental parameters and measurements and may include a rotary encoder for measuring animal locomotion on a running wheel, an infrared camera and light source for pupil/face measurements, and stimulus presentation equipment (Ozgur et al., 2023). At a minimum, a lick spout and lick detection circuit must be built to deliver ethanol and record lick rates (Williams et al., 2018). Here, we use an Arduino UNO microcontroller to interface with MATLAB on the main experimental computer. Thus, despite the need for construction of a head-fixation rig and ethanol delivery circuit, the overall cost for HFD is considerably lower than many commercial behavioral systems.

A third, obvious limitation is the fact that the animal's head is immobilized, which introduces potential confounds relating to stress levels (Juczewski et al., 2020). There are several ways to reduce stress associated with head-fixation (Barkus et al., 2022). The first method, employed here, is to habituate animals to handling and head-fixation. Habituation can limit the effect of these stimuli on the animal's stress state, but of course this requires consistent exposure to the same experimental rig and/or experimenter. The number of habituation sessions can range from several days to several weeks depending on how important it is to reduce head-fixed stress for the experimental question (Juczewski et al., 2020; Russo et al., 2021). Furthermore, providing a running wheel allows mice to move even when the head is stationary. This can be achieved using either a flat disk or a light sphere levitating on air. Additionally, stress can be reduced by providing a dark, sound-dampened enclosure that separates the animal from the experimenter and limits visual, auditory, and olfactory stimuli that may induce stress responses. In addition to preventative measures for mitigating stress, quantifying the degree to which head-fixation affects different animals may help control for stress as a source of behavioral and physiological variability. In addition to measuring pupil dynamics and locomotion, blood samples can be acquired to assay for circulating stress hormones. In this way, heterogeneity in drinking behavior and physiology can be mapped onto potential differences in stress response to head fixation.

4.5. Specific limitations of this head-fixed drinking paradigm

In addition to the above general limitations with head-fixed paradigms, there are several limitations in our current work that should be addressed in future studies. Our main goal was to test the conditions under which mice maintained on an *ad libitum* water and food schedule consume ethanol during head-fixation. Mice were given 4 days in the head-fixed drinking paradigm, which was sufficient for observing binge-like ethanol intake levels in most subjects (Fig. 1F). However, the current paradigm poses some challenges in interpreting ACC neuronal recordings, especially during the pre-drinking period. We opted to include a pre-drinking period to allow comparison of activity during baseline and during/after ethanol consumption. However, with limited training, it is unclear when mice differentiate that ethanol is only available in the drinking blocks and not during the pre-drinking block. Hence, the activity recorded during the pre-drinking period may reflect not only the baseline activity of neurons but also additional factors like expectation that could vary within individual HFD sessions and across days of HFD. We note that this challenge is not unique to our work since defining a baseline period is generally difficult in neuronal recordings made in awake, behaving animals. In the current work, we addressed this concern by restricting analysis of activity changes to only the drinking period in addition to comparing pre-drinking and drinking activity levels. In the future, it will be important to train mice for a longer period on the paradigm to better interpret neuronal activity during the pre-drinking period. In addition, it may be useful to explicitly cue the drinking period, for example by automatically extending the spout so it is within licking distance only during the drinking period or presenting a light cue for the duration of the drinking period. A post-drinking recording period should also be added, which would allow cleaner examination of the intoxicating effect of ethanol on neuronal activity without the confound of concurrent ethanol deliveries and consummatory licking.

Another issue is the action-outcome contingency employed in this paradigm. In home cage drinking, each lick delivers a drop of ethanol, allowing for important insights regarding motivation and the drive to drink by detailed analysis of licking microstructure and the underlying neuronal activity (Darevsky et al., 2019; Renteria et al., 2020; Starski et al., 2023). In our paradigm, ethanol delivery is only partially under the animal's control, requiring one lick since the last delivery for additional drops to be available and only after a pseudorandom time delay. We implemented this design mainly to account for a limitation with calcium imaging. Calcium imaging has lower temporal resolution than other methods like voltage imaging or electrophysiology, making it challenging to analyze heterogeneous population activity in rapidly evolving behavior such as would be the case if mice could trigger multiple drops of ethanol in close succession. We chose to have a pseudorandom delay between ethanol drop deliveries to both gauge ongoing animal engagement with ethanol consumption (by intermittent delivery after licking) and temporally separate drinking activity to accurately quantify potential phasic responses to ethanol. Future work should explore further refinements to the paradigm to better align action-outcome contingencies between head-fixed and freely moving home cage drinking by implementing a 1-to-1 lick-ethanol drop contingency. Importantly, by demonstrating that head-fixed mice do voluntarily consume ethanol, our work paves the way for future behavioral tasks with diverse action-outcome contingencies, including operant responding with lever press or pavlovian conditioning, that would allow for independent assessment of important factors such as motivation, learning, and expectation.

4.6. ACC activity during ethanol consumption

Here, we demonstrate that one experimental advantage of HFD is to apply two-photon microscopy to studying the heterogeneity of neuronal activity during epochs of alcohol consumption. We find that level acute ethanol intoxication does not significantly affect neuronal activity of single neurons at the population level, at least when activity rates are compared during pre-drinking and the last 10 min of drinking (Fig. 7A and B). At the same time, mean-session activity (i.e., the average activity of all simultaneously recorded single neurons) tracked the number of ethanol drops delivered in 2-min bin. This correlation remained intact after removing neuronal activity during the consummatory period, suggesting that the relationship between population activity and ethanol delivery/receipt is at least partly dissociable from licking behavior and related consummatory processes (Fig. 8A and B; Supp. Figs. 2A and B). From the current experiments, we are not able to determine what this relationship between ACC activity and ethanol deliveries reflects. Speculatively, it may represent rewarding or motivational factors related to ethanol consumption. Whether this relationship is specific for ethanol consumption or generally consumption of other rewarding liquids like sucrose awaits further studies and will provide additional

insights.

We also found that alcohol affects the tonic level of activity in subsets of L2/3 excitatory neurons in the ACC that show either increased or decreased activity across ethanol consumption (Fig. 7C–F). Surprisingly, the population proportions of these subsets are relatively similar and the population average firing rate does not significantly change with ethanol consumption. This observation corroborates previous work in the rat prefrontal cortex using *in vivo* electrophysiology demonstrating significant heterogeneity of neuronal excitability in response to ethanol exposure using *in vivo* electrophysiology but no average change in firing rate at the population level (Linsenbardt and Lapish, 2015; Morningstar et al., 2020). We also found similar heterogeneity in phasic neuronal responses, both positive and negative, to the delivery of alcohol, which may also represent licking activity, ethanol valence, behavioral and autonomic arousal, and/or other consumption-related processes (Fig. 8F–K). Further work is needed to map the heterogeneity of these responses to animal consummatory behavior including measures of sympathetic outflow.

The individual heterogeneity of ACC neuron activity in response to HFD could represent a broader change in population dynamics. Though we did not see an overall effect of ethanol consumption on firing rates (Fig. 7A), the correlated activity across the population could potentially be affected. By comparing the pair-wise correlations between neuron pairs during pre-drinking and drinking, we did not detect a significant change when considering all recorded neurons (Fig. 9C). However, neurons with increased tonic and phasic activity showed higher pair-wise correlations during drinking as compared to the pre-drinking period (Fig. 9D,F). For neurons with increased phasic activity, this effect may partly be driven by consummatory process, since the change in correlation was lost after removing activity 10s after ethanol deliveries (Supp. Fig. 5D). This suggests that in addition to having no net effect on firing rates, ethanol consumption does not drastically affect neuronal correlations in L2/3 of the mouse ACC. These mice only had a limited exposure history and it is possible that repeated ethanol consumption may more severely affect activity levels and correlations. Alternatively, these findings may point to systems-level mechanisms that homeostatically maintain neuronal activity and correlations within a narrow setpoint and confer resiliency against large changes in activity levels.

4.7. Advantages of combined head-fixed drinking and two-photon calcium imaging

A benefit of HFD and two-photon microscopy is the ability to longitudinally track individual neurons across days or weeks. Here, we analyzed single sessions across animals. Future experiments are needed to determine whether the individual firing rates and population correlations are stable over multiple sessions within the same animal (e.g., do neurons with increased firing rates in response to HFD show the same effect across days?). By tracking ethanol consumption and neuronal physiology longitudinally, cortical activity signatures may predict variable ethanol consumption within animals.

Another benefit of HFD and two-photon microscopy is the ability to quantify activity in genetically identified (e.g., cell-type specific expression of calcium indicators) or anatomically identified (e.g., anterograde/retrograde traces) subpopulations of neurons. This cell-type specific imaging can be combined with cell-type specific full-field or single-cell optogenetics (Packer et al., 2015), which would allow experimenters to first record activity during ethanol consumption, and then stimulate or silence subsets of those neurons to investigate their contribution to physiology and behavior. We limited our analysis to CaMKII-expressing cells, which are predominantly excitatory in the cortex. However, increasing evidence suggests that inhibitory neuronal subtypes play important roles in the development of drinking behavior in the cortex (Dao et al., 2021; Fish and Joffe, 2022; Patton et al., 2023). By using dual-color calcium indicators, both excitatory and inhibitory populations can be simultaneously imaged using two-photon and HFD. Future work is needed to track the temporal evolution of these populations with the acquisition and maintenance of ethanol drinking behavior. Overall, we believe the HFD paradigm complements freely moving paradigms, allowing alcohol studies using activity recording and manipulation techniques not readily available in other models.

Data and code availability

Data and analysis code will be made available by the corresponding author upon request.

CRediT authorship contribution statement

Anagha Kalelkar: Investigation, Software, Validation. **Grayson Sipe:** Conceptualization, Methodology, Investigation, Writing – original draft, Writing – review & editing, Visualization, Funding acquisition. **Ana Raquel Castro E Costa:** Investigation. **Ilka M. Lorenzo:** Investigation. **My Nguyen:** Investigation. **Ivan Linares-Garcia:** Software. **Elena Vazey:** Methodology, Funding acquisition. **Rafiq Huda:** Conceptualization, Methodology, Software, Formal analysis, Resources, Writing – original draft, Writing – review & editing, Visualization, Supervision, Project administration, Funding acquisition.

Declaration of competing interest

The authors declare that they have no known competing financial interests or personal relationships that could have appeared to influence the work reported in this paper.

Data availability

Data will be made available on request.

Acknowledgements

This work was supported by grants from the National Institute of Mental Health (R00MH112855 to R.H.), NARSAD Young Investigator Award (R.H.), National Institute on Alcohol Abuse and Alcoholism (K99AA028579 to G.O.S. and U01-AA025481 to E.M.V.), and Office of the Director, National Institutes of Health (R01-AA030594 to R.H.).

Appendix A. Supplementary data

Supplementary data to this article can be found online at https://doi.org/10.1016/j.neuropharm.2023.109800.

References

Accanto, N., Blot, F.G.C., Lorca-Camara, A., Zampini, V., Bui, F., Tourain, C., Badt, N., Katz, O., Emiliani, V., 2023. A flexible two-photon fiberscope for fast activity imaging and precise optogenetic photostimulation of neurons in freely moving mice. Neuron 111, 176–189 e176.

Alexander, W.H., Brown, J.W., 2011. Medial prefrontal cortex as an action-outcome predictor. Nat. Neurosci. 14, 1338–1344.

Ardinger, C.E., Lapish, C.C., Czachowski, C.L., Grahame, N.J., 2022. A critical review of front-loading: a maladaptive drinking pattern driven by alcohol's rewarding effects. Alcohol Clin. Exp. Res. 46, 1772–1782.

Barkus, C., Bergmann, C., Branco, T., Carandini, M., Chadderton, P.T., Galinanes, G.L., Gilmour, G., Huber, D., Huxter, J.R., Khan, A.G., King, A.J., Maravall, M., O'Mahony, T., Ragan, C.I., Robinson, E.S.J., Schaefer, A.T., Schultz, S.R., Sengpiel, F., Prescott, M.J., 2022. Refinements to rodent head fixation and fluid/food control for neuroscience. J. Neurosci. Methods 381, 109705.

Bechara, A., Dolan, S., Denburg, N., Hindes, A., Anderson, S.W., Nathan, P.E., 2001. Decision-making deficits, linked to a dysfunctional ventromedial prefrontal cortex, revealed in alcohol and stimulant abusers. Neuropsychologia 39, 376–389.

Bloem, B., Huda, R., Sur, M., Graybiel, A.M., 2017. Two-photon imaging in mice shows striosomes and matrix have overlapping but differential reinforcement-related responses. Elife 6.
Breton-Provencher, V., Drummond, G.T., Feng, J., Li, Y., Sur, M., 2022. Spatiotemporal dynamics of noradrenaline during learned behaviour. Nature. 606 (7915), 732–738.
Cannady, R., Nguyen, T., Padula, A.E., Rinker, J.A., Lopez, M.F., Becker, H.C., Woodward, J.J., Mulholland, P.J., 2021. Interaction of chronic intermittent ethanol and repeated stress on structural and functional plasticity in the mouse medial prefrontal cortex. Neuropharmacology 182, 108396.
Cannady, R., Nimitvilai-Roberts, S., Jennings, S.D., Woodward, J.J., Mulholland, P.J., 2020. Distinct region- and time-dependent functional cortical adaptations in C57BL/6J mice after short and prolonged alcohol drinking. eNeuro 7.
Carlsen, E.M.M., Nedergaard, M., Rasmussen, R.N., 2022. Versatile treadmill system for measuring locomotion and neural activity in head-fixed mice. STAR Protoc. 3, 101701.
Chen, T.-W., Wardill, T.J., Sun, Y., Pulver, S.R., Renninger, S.L., Baohan, A., Schreiter, E. R., Kerr, R.A., Orger, M.B., Jayaraman, V., Looger, L.L., Svoboda, K., Kim, D.S., 2013. Ultrasensitive fluorescent proteins for imaging neuronal activity. Nature 499, 295.
Cohen, M.R., Kohn, A., 2011. Measuring and interpreting neuronal correlations. Nat. Neurosci. 14, 811–819.
Crabbe, J.C., Harris, R.A., Koob, G.F., 2011. Preclinical studies of alcohol binge drinking. Ann. N. Y. Acad. Sci. 1216, 24–40.
Dao, N.C., Brockway, D.F., Suresh Nair, M., Sicher, A.R., Crowley, N.A., 2021. Somatostatin neurons control an alcohol binge drinking prelimbic microcircuit in mice. Neuropsychopharmacology 46 (11), 1906–1917.
Darevsky, D., Gill, T.M., Vitale, K.R., Hu, B., Wegner, S.A., Hopf, F.W., 2019. Drinking despite adversity: behavioral evidence for a head down and push strategy of conflict-resistant alcohol drinking in rats. Addiction Biol. 24, 426–437.
Dawson, D.A., Grant, B.F., Li, T.K., 2005. Quantifying the risks associated with exceeding recommended drinking limits. Alcohol Clin. Exp. Res. 29, 902–908.
Fish, K.N., Joffe, M.E., 2022. Targeting prefrontal cortex GABAergic microcircuits for the treatment of alcohol use disorder. Front. Synaptic Neurosci. 14, 936911.
George, O., Koob, G.F., 2010. Individual differences in prefrontal cortex function and the transition from drug use to drug dependence. Neurosci. Biobehav. Rev. 35, 232–247.
Giacometti, L.L., Chandran, K., Figueroa, L.A., Barker, J.M., 2020. Astrocyte modulation of extinction impairments in ethanol-dependent female mice. Neuropharmacology 179, 108272.
Gioia, D.A., Woodward, J.J., 2021. Altered activity of lateral Orbitofrontal cortex neurons in mice following chronic intermittent ethanol exposure. eNeuro 8.
Goldstein, R.Z., Volkow, N.D., 2011. Dysfunction of the prefrontal cortex in addiction: neuroimaging findings and clinical implications. Nat. Rev. Neurosci. 12, 652–669.
Gordon-Fennell, A., Barbakh, J.M., Utley, M.T., Singh, S., Bazzino, P., Gowrishankar, R., Bruchas, M.R., Roitman, M.F., Stuber, G.D., 2023. An open-source platform for head-fixed operant and consummatory behavior. Elife 12.
Halladay, L.R., Kocharian, A., Piantadosi, P.T., Authement, M.E., Lieberman, A.G., Spitz, N.A., Coden, K., Glover, L.R., Costa, V.D., Alvarez, V.A., Holmes, A., 2020. Prefrontal regulation of punished ethanol self-administration. Biol. Psychiatr. 87, 967–978.
Harrison, N.L., Skelly, M.J., Grosserode, E.K., Lowes, D.C., Zeric, T., Phister, S., Salling, M.C., 2017. Effects of acute alcohol on excitability in the CNS. Neuropharmacology 122, 36–45.
Holleran, K.M., Winder, D.G., 2017. Preclinical voluntary drinking models for alcohol abstinence-induced affective disturbances in mice. Gene Brain Behav. 16, 8–14.
Holtmaat, A., de Paola, V., Wilbrecht, L., Trachtenberg, J.T., Svoboda, K., Portera-Cailliau, C., 2012. Imaging neocortical neurons through a chronic cranial window, 2012 Cold Spring Harb. Protoc. 694–701.
Huda, R., Sipe, G.O., Breton-Provencher, V., Cruz, K.G., Pho, G.N., Adam, E., Gunter, L. M., Sullins, A., Wickersham, I.R., Sur, M., 2020. Distinct prefrontal top-down circuits differentially modulate sensorimotor behavior. Nat. Commun. 11, 6007.
Huynh, N., Arabian, N.M., Asatryan, L., Davies, D.L., 2019. Murine drinking models in the development of pharmacotherapies for alcoholism: drinking in the dark and two-bottle choice. J. Vis. Exp.
Jedema, H.P., Carter, M.D., Dugan, B.P., Gurnsey, K., Olsen, A.S., Bradberry, C.W., 2011. The acute impact of ethanol on cognitive performance in rhesus macaques. Cerebr. Cortex 21, 1783–1791.
Ji, N., Freeman, J., Smith, S.L., 2016. Technologies for imaging neural activity in large volumes. Nat. Neurosci. 19, 1154–1164.
Juavinett, A.L., Bekheet, G., Churchland, A.K., 2019. Chronically implanted Neuropixels probes enable high-yield recordings in freely moving mice. Elife 8.
Juczewski, K., Koussa, J.A., Kesner, A.J., Lee, J.O., Lovinger, D.M., 2020. Stress and behavioral correlates in the head-fixed method: stress measurements, habituation dynamics, locomotion, and motor-skill learning in mice. Sci. Rep. 10, 12245.
Kohn, A., Coen-Cagli, R., Kanitscheider, I., Pouget, A., 2016. Correlations and neuronal population information. Annu. Rev. Neurosci. 39, 237–256.
Lee, J.J., Krumin, M., Harris, K.D., Carandini, M., 2022. Task specificity in mouse parietal cortex. Neuron 110, 2961–2969 e2965.
Linsenbardt, D.N., Lapish, C.C., 2015. Neural firing in the prefrontal cortex during alcohol intake in alcohol-preferring "P" versus wistar rats. Alcohol Clin. Exp. Res. 39, 1642–1653.
Liu, Y., Jean-Richard-Dit-Bressel, P., Yau, J.O., Willing, A., Prasad, A.A., Power, J.M., Killcross, S., Clifford, C.W.G., McNally, G.P., 2020. The mesolimbic dopamine activity signatures of relapse to alcohol-seeking. J. Neurosci. 40, 6409–6427.
Liu, Z., Lu, X., Villette, V., Gou, Y., Colbert, K.L., Lai, S., Guan, S., Land, M.A., Lee, J., Assefa, T., Zollinger, D.R., Korympidou, M.M., Vlasits, A.L., Pang, M.M., Su, S., Cai, C., Froudarakis, E., Zhou, N., Patel, S.S., Smith, C.L., Ayon, A., Bizouard, P., Bradley, J., Franke, K., Clandinin, T.R., Giovannucci, A., Tolias, A.S., Reimer, J., Dieudonne, S., St-Pierre, F., 2022. Sustained deep-tissue voltage recording using a fast indicator evolved for two-photon microscopy. Cell.
Lu, Y.L., Richardson, H.N., 2014. Alcohol, stress hormones, and the prefrontal cortex: a proposed pathway to the dark side of addiction. Neuroscience 277, 139–151.
Manita, S., Shigetomi, E., Bito, H., Koizumi, S., Kitamura, K., 2022. In vivo wide-field and two-photon calcium imaging from a mouse using a large cranial window. J. Vis. Exp. 186, e64224.
McCool, B.A., 2011. Ethanol modulation of synaptic plasticity. Neuropharmacology 61, 1097–1108.
Morningstar, M.D., Linsenbardt, D.N., Lapish, C.C., 2020. Ethanol alters variability, but not rate, of firing in medial prefrontal cortex neurons of awake-behaving rats. Alcohol Clin. Exp. Res. 44 (11), 2225–2238.
Nath, T., Mathis, A., Chen, A.C., Patel, A., Bethge, M., Mathis, M.W., 2019. Using DeepLabCut for 3D markerless pose estimation across species and behaviors. Nat. Protoc. 14, 2152–2176.
O'Connor, D.H., Clack, N.G., Huber, D., Komiyama, T., Myers, E.W., Svoboda, K., 2010. Vibrissa-based object localization in head-fixed mice. J. Neurosci. 30, 1947–1967.
Ottenheimer, D.J., Hjort, M.M., Bowen, A.J., Steinmetz, N.A., Stuber, G.D., 2023. A stable, distributed code for cue value in mouse cortex during reward learning. Elife 12.
Ozgur, A., Park, S.B., Flores, A.Y., Oijala, M., Lur, G., 2023. A comprehensive, affordable, open-source hardware-software solution for flexible implementation of complex behaviors in head-fixed mice. eNeuro 10.
Pachitariu, M., Stringer, C., Dipoppa, M., Schröder, S., Rossi, L.F., Dalgleish, H., Carandini, M., Harris, K.D., 2017. Suite2p: beyond 10,000 neurons with standard two-photon microscopy. BioRxiv, 061507.
Packer, A.M., Russell, L.E., Dalgleish, H.W., Hausser, M., 2015. Simultaneous all-optical manipulation and recording of neural circuit activity with cellular resolution in vivo. Nat. Methods 12, 140–146.
Patrick, M.E., Azar, B., 2018. High-intensity drinking. Alcohol. Res. 39, 49–55.
Patton, M.S., Sheats, S.H., Siclair, A.N., Mathur, B.N., 2023. Alcohol potentiates multiple GABAergic inputs to dorsal striatum fast-spiking interneurons. Neuropharmacology, 109527.
Pava, M.J., Woodward, J.J., 2014. Chronic ethanol alters network activity and endocannabinoid signaling in the prefrontal cortex. Front. Integr. Neurosci. 8, 58.
Prencipe, L., Iaccheri, E., Manzati, C., 1987. Enzymic ethanol assay: a new colorimetric method based on measurement of hydrogen peroxide. Clin. Chem. 33, 486–489.
Radke, A.K., Sneddon, E.A., Frasier, R.M., Hopf, F.W., 2021. Recent perspectives on sex differences in compulsion-like and binge alcohol drinking. Int. J. Mol. Sci. 22.
Renteria, R., Cazares, C., Gremel, C.M., 2020. Habitual ethanol seeking and licking microstructure of enhanced ethanol self-administration in ethanol-dependent mice. Alcohol Clin. Exp. Res. 44, 880–891.
Rhodes, J.S., Best, K., Belknap, J.K., Finn, D.A., Crabbe, J.C., 2005. Evaluation of a simple model of ethanol drinking to intoxication in C57BL/6J mice. Physiol. Behav. 84, 53–63.
Ridderinkhof, K.R., de Vlugt, Y., Bramlage, A., Spaan, M., Elton, M., Snel, J., Band, G.P., 2002. Alcohol consumption impairs detection of performance errors in mediofrontal cortex. Science 298, 2209–2211.
Rinker, J.A., Marshall, S.A., Mazzone, C.M., Lowery-Gionta, E.G., Gulati, V., Pleil, K.E., Kash, T.L., Navarro, M., Thiele, T.E., 2017. Extended amygdala to ventral tegmental area corticotropin-releasing factor circuit controls binge ethanol intake. Biol. Psychiatr. 81, 930–940.
Robinson, S.L., Marrero, I.M., Perez-Heydrich, C.A., Sepulveda-Orengo, M.T., Reissner, K.J., Thiele, T.E., 2019. Medial prefrontal cortex neuropeptide Y modulates binge-like ethanol consumption in C57BL/6J mice. Neuropsychopharmacology 44, 1132–1140.
Russo, G., Helluy, X., Behroozi, M., Manahan-Vaughan, D., 2021. Gradual restraint habituation for awake functional magnetic resonance imaging combined with a sparse imaging paradigm reduces motion artifacts and stress levels in rodents. Front. Neurosci. 15, 805679.
Salling, M.C., Skelly, M.J., Avegno, E., Regan, S., Zeric, T., Nichols, E., Harrison, N.L., 2018. Alcohol consumption during adolescence in a mouse model of binge drinking alters the intrinsic excitability and function of the prefrontal cortex through a reduction in the hyperpolarization-activated cation current. J. Neurosci. 38, 6207–6222.
Siciliano, C.A., Calipari, E.S., Cuzon Carlson, V.C., Helms, C.M., Lovinger, D.M., Grant, K. A., Jones, S.R., 2015. Voluntary ethanol intake predicts kappa-opioid receptor supersensitivity and regionally distinct dopaminergic adaptations in macaques. J. Neurosci. 35, 5959–5968.
Siciliano, C.A., Tye, K.M., 2019. Leveraging calcium imaging to illuminate circuit dysfunction in addiction. Alcohol 74, 47–63.
Simms, J.A., Steensland, P., Medina, B., Abernathy, K.E., Chandler, L.J., Wise, R., Bartlett, S.E., 2008. Intermittent access to 20% ethanol induces high ethanol consumption in Long-Evans and Wistar rats. Alcohol Clin. Exp. Res. 32, 1816–1823.
Slotnick, B., 2009. A simple 2-transistor touch or lick detector circuit. J. Exp. Anal. Behav. 91, 253–255.
Sprow, G.M., Thiele, T.E., 2012. The neurobiology of binge-like ethanol drinking: evidence from rodent models. Physiol. Behav. 106, 325–331.
Starski, P.A., Sergio, T.D.O., Hopf, F.W., 2023. Using lickometry to infer differential contributions of salience network regions during compulsion-like alcohol drinking. Addict. Neurosci. 7, 100102.
Steinmetz, N.A., Koch, C., Harris, K.D., Carandini, M., 2018. Challenges and opportunities for large-scale electrophysiology with Neuropixels probes. Curr. Opin. Neurobiol. 50, 92–100.

Thiele, T.E., Crabbe, J.C., Boehm 2nd, S.L., 2014. "Drinking in the Dark" (DID): a simple mouse model of binge-like alcohol intake, 9 49 41-12 Curr. Protoc. Neurosci. 68.
Thiele, T.E., Navarro, M., 2014. "Drinking in the dark" (DID) procedures: a model of binge-like ethanol drinking in non-dependent mice. Alcohol 48, 235–241.
Tian, H., Davis, H.C., Wong-Campos, J.D., Park, P., Fan, L.Z., Gmeiner, B., Begum, S., Werley, C.A., Borja, G.B., Upadhyay, H., Shah, H., Jacques, J., Qi, Y., Parot, V., Deisseroth, K., Cohen, A.E., 2023. Video-based pooled screening yields improved far-red genetically encoded voltage indicators. Nat. Methods. 20, 1082–1094.
Vollmer, K.M., Doncheck, E.M., Grant, R.I., Winston, K.T., Romanova, E.V., Bowen, C.W., Siegler, P.N., Green, L.M., Bobadilla, A.C., Trujillo-Pisanty, I., Kalivas, P.W., 2021. A novel assay allowing drug self-administration, extinction, and reinstatement testing in head-restrained mice. Front. Behav. Neurosci. 15, 744715.
Vollmer, K.M., Green, L.M., Grant, R.I., Winston, K.T., Doncheck, E.M., Bowen, C.W., Paniccia, J.E., Clarke, R.E., Tiller, A., Siegler, P.N., Bordieanu, B., Siemsen, B.M., Denton, A.R., Westphal, A.M., Jhou, T.C., Rinker, J.A., McGinty, J.F., Scofield, M.D., Otis, J.M., 2022. An opioid-gated thalamoaccumbal circuit for the suppression of reward seeking in mice. Nat. Commun. 13, 6865.
Wilcox, C.E., Dekonenko, C.J., Mayer, A.R., Bogenschutz, M.P., Turner, J.A., 2014. Cognitive control in alcohol use disorder: deficits and clinical relevance. Rev. Neurosci. 25, 1–24.
Williams, B., Speed, A., Haider, B., 2018. A novel device for real-time measurement and manipulation of licking behavior in head-fixed mice. J. Neurophysiol. 120, 2975–2987.
Timme, N.M., Ardinger, C.E., Weir, S.D.C., Zelaya-Escobar, R., Kruger, R., Lapish, C.C., 2024. Non-consummatory behavior signals predict aversion-resistant alcohol drinking in head-fixed mice. Neuropharmacology 242, 109762.